PTEP

Prog. Theor. Exp. Phys. **2023** 123A01(28 pages)
DOI: 10.1093/ptep/ptad138

Real eigenvector distributions of random tensors with backgrounds and random deviations

Naoki Sasakura [1,2,⋆]

[1] *Yukawa Institute for Theoretical Physics, Kyoto University, Kitashirakawa, Sakyo-ku, Kyoto 606-8502, Japan*

[2] *CGPQI, Yukawa Institute for Theoretical Physics, Kyoto University, Kitashirakawa, Sakyo-ku, Kyoto 606-8502, Japan*

⋆E-mail: sasakura@yukawa.kyoto-u.ac.jp

Received November 2, 2023; Accepted November 14, 2023; Published November 15, 2023

As in random matrix theories, eigenvector/value distributions are important quantities of random tensors in their applications. Recently, real eigenvector/value distributions of Gaussian random tensors have been explicitly computed by expressing them as partition functions of quantum field theories with quartic interactions. This procedure to compute distributions in random tensors is general, powerful, and intuitive, because one can take advantage of well-developed techniques and knowledge of quantum field theories. In this paper we extend the procedure to the cases that random tensors have mean backgrounds and eigenvector equations have random deviations. In particular, we study in detail the case that the background is a rank-one tensor, namely, the case of a spiked tensor. We discuss the condition under which the background rank-one tensor has a visible peak in the eigenvector distribution. We obtain a threshold value, which agrees with a previous result in the literature.

Subject Index A13, A45, B83, B86

1. Introduction

Eigenvalue distributions are important quantities in random matrix models. The most well-known is the Wigner semi-circle law of the eigenvalue distribution, which models energy spectra of strongly interacting many-body systems [1]. Eigenvalue distributions are also used as an important technique in solving matrix models [2,3]. Topological changes of eigenvalue distributions provide insights into the quantum chromodynamics [4,5].

It would be natural to ask how such knowledge about random matrices can be generalized to random tensors. Random tensor models [6–9] were originally introduced to extend random matrix models, which are successful as 2D quantum gravity, to higher-dimensional quantum gravity. Recently random tensor models have also played interesting roles in various other subjects (see, e.g. Ref. [10]). While physically interesting matrices like the hermitian can be one-to-one mapped to sets of eigenvalues by symmetry transformations, this cannot be done in general for tensors. However, we sometimes encounter what we may call tensor eigenvectors/values [11–14] in studies. A well-known example is the distribution of the energy spectra of the spherical p-spin model [15,16] for spin glasses, which was comprehensively analyzed in Ref. [17]. In fact, this is the same problem as obtaining the real eigenvalue[1] distribution of a real symmetric ran-

[1]More precisely, they are Z-eigenvalues in the terminology of Refs. [11,14].

dom tensor. Tensor eigenvector/value problems also appear in other contexts, such as anti-de Sitter/conformal field theory (AdS/CFT) [18], classical gravitational systems [19], and applied mathematics for technologies [14].

Considering their broad appearance, it is worth effort to systematically understand properties of tensor eigenvectors/values. Our focus is on their distributions for Gaussian random tensors. Some interesting results have already been obtained in the literature. In Refs. [20,21] the expectation values of numbers of real eigenvalues of random tensors were computed. In Ref. [22] the maximum eigenvalues of random tensors were estimated in the large-N limit.[2] In Ref. [23], the Wigner semi-circle law was extended to a form for random tensors. In Refs. [24–26] the present author computed real eigenvalue distributions of random tensors by quantum field theoretical methods.

In the last works above by the present author, the procedure is to first rewrite the eigenvector problems as partition functions of quantum field theories with quartic interactions, and then to compute the partition functions. There are some merits in this procedure; it is general, powerful, and intuitive. As far as tensors have Gaussian distributions, one can in principle extend the procedure to obtain quantum field theories of quartic interactions for a wide range of other tensor problems, such as complex eigenvalue/vector distributions, tensor rank decompositions, etc. Then, once such quantum field theories have been obtained, one can use various well-developed quantum field theoretical techniques, such as Schwinger–Dyson equations as in Ref. [25]. Moreover, it is generally more intuitive to compute partition functions than to directly treat systems of eigenvector/value polynomial equations. For instance, in the large-N analysis of Ref. [25], there exists a phase transition point between perturbative and nonperturbative regimes of the quantum field theory, and this point corresponds to the edge of the eigenvalue distribution.

The purpose of the present paper is to apply this quantum field theoretical procedure to a slightly different setup than the previous works [24–26]. We assume the random tensors have mean values, namely, backgrounds. This is a useful setup in the research of data analysis, in which backgrounds are signals and deviations around them are noises [27]. It is an important question under what conditions signals can be recovered from data contaminated by noises [27–29]. We also introduce random deviations to eigenvector equations.[3] This simulates solving approximately eigenvector equations, e.g. by the Monte Carlo (MC) method or simulated annealing. As we will see, also in this generalized setup, the distributions can be rewritten as partition functions of quantum field theories with quartic interactions, and the partition functions can be computed explicitly, even exactly in some cases.

This paper is organized as follows. In Sect. 2, we introduce a real eigenvector equation with a tensor mean background and deviations to the equation, and obtain an integral expression of the eigenvector distribution. In Sect. 3, we derive the quantum field theory expressing a "signed" distribution of the eigenvectors. This distribution is not authentic but is weighted with an extra sign associated to each eigenvector. This distribution is easier to compute, because the quantum field theory contains only a pair of fermions. In particular, when the background is taken to be a rank-one tensor (a spiked tensor), we obtain an exact expression of the distribution in terms of hypergeometric functions. In Sect. 4 we derive the quantum field theory expression of the

[2]Throughout this paper, N denotes the range of indices of tensors, namely, an index takes values, 1, 2, ···, N.

[3]This particular case will also be analyzed in detail in Ref. [30].

(authentic) distribution of the eigenvectors. In particular we explicitly derive the distribution for the spiked tensor case by using an approximation taking advantage of the quantum field theoretical expression. In Sect. 5, we compare the expressions of the distributions obtained in the previous sections with MC simulations. We obtain very good agreement, including for the case treated by the approximation. In Sect. 6, we consider the large-N limit, especially paying attention to whether the rank-one tensor background has a visible peak in the distributions. We derive the scaling and the range of parameters in which this happens. The threshold value is shown to agree with that of Ref. [29]. The last section is devoted to a summary and future prospects.

2. Real tensor eigenvector equation with backgrounds and deviations

In this paper we restrict ourselves to order-three tensors[4] for simplicity. We consider the following eigenvector equation [11–14] with a background tensor Q and a deviation vector η,

$$(Q_{abc} + C_{abc})v_b v_c = v_a + \eta_a. \tag{1}$$

Here the indices take $a, b, c = 1, 2, \ldots, N$, and repeated indices are assumed to be summed over unless otherwise stated throughout this paper. We assume that Q, C are real symmetric order-three tensors and v, η are real vectors:

$$\begin{aligned} &Q_{abc} = Q_{bac} = Q_{bca} \in \mathbb{R}, \\ &C_{abc} = C_{bac} = C_{bca} \in \mathbb{R}, \\ &v_a,\ \eta_a \in \mathbb{R}. \end{aligned} \tag{2}$$

While Q is an externally given background tensor, C_{abc} is a random tensor with Gaussian distribution of a zero mean value. The vector η describes a deviation of the eigenvector equation, and is a random real vector with Gaussian distribution of a zero mean value. We will compute the distributions of v, namely the distributions of the real "eigenvector" solutions to Eq. (1). Note that, if we ignore the background Q and the deviation η, the setup goes back to the cases previously studied in Refs. [24–26].

For given Q, C, η, the distribution of v is given by

$$\begin{aligned} \rho(v, Q, C, \eta) &= \sum_{i=1}^{\#\mathrm{sol}(Q,C,\eta)} \prod_{a=1}^{N} \delta\left(v_a - v_a^i\right) \\ &= |\det M(v, Q, C)| \prod_{a=1}^{N} \delta\left(v_a + \eta_a - (Q_{abc} + C_{abc})v_b v_c\right) \end{aligned} \tag{3}$$

where v^i $(i = 1, 2, \ldots, \#\mathrm{sol}(Q, C, \eta))$ are all the real solutions to Eq. (1), and $|\det M(v, Q, C)|$ is the absolute value of the determinant of the matrix,

$$M(v, Q, C)_{ab} = \frac{\partial}{\partial v_a}\left(v_b + \eta_b - (Q_{bcd} + C_{bcd})v_c v_d\right) = \delta_{ab} - 2(Q_{abc} + C_{abc})v_c, \tag{4}$$

which is the Jacobian factor associated to the change of the variables of the delta functions in Eq. (3).

[4] Namely, tensors have three indices.

When C, η have Gaussian distributions with zero mean values, the eigenvector distributions are computed by taking the average over C, η:

$$\rho(v,Q,\beta)=\langle\rho(v,Q,C,\eta)\rangle_{C,\eta}$$
$$=\frac{1}{AA'}\int_{\mathbb{R}^{\#C}}dC\int_{\mathbb{R}^N}d\eta\, e^{-\alpha C^2-\frac{1}{4\beta}\eta^2}\,|\det M(v,Q,C)|$$
$$\cdot\prod_{a=1}^{N}\delta\left(v_a+\eta_a-(Q_{abc}+C_{abc})v_bv_c\right),\qquad(5)$$

where $\alpha,\beta>0$, $\#C$ is the number[5] of the independent components of C, $C^2=C_{abc}C_{abc}$, $\eta^2=\eta_a\eta_a$, $A=\int_{\mathbb{R}^{\#C}}dC\,e^{-\alpha C^2}$, and $A'=\int_{\mathbb{R}^N}d\eta\,e^{-\frac{1}{4\beta}\eta^2}$. Here a slightly complicated introduction of β is for later convenience. By using the well-known formula, $\frac{1}{2\pi}\int_{\mathbb{R}}d\lambda\,e^{i\lambda x}=\delta(x)$, the integration of the delta functions over η in Eq. (5) can be rewritten as

$$\frac{1}{A'}\int_{\mathbb{R}^N}d\eta\,e^{-\frac{1}{4\beta}\eta^2}\prod_{a=1}^{N}\delta\left(v_a+\eta_a-(Q_{abc}+C_{abc})v_bv_c\right)=\frac{1}{(2\pi)^N}\int_{\mathbb{R}^N}d\lambda\,e^{-\beta\lambda^2+i\lambda_a(v_a-(Q_{abc}+C_{abc})v_bv_c)}.\qquad(6)$$

Therefore, by putting this into Eq. (5), we obtain

$$\rho(v,Q,\beta)=\frac{1}{(2\pi)^NA}\int_{\mathbb{R}^{\#C}}dC\int_{\mathbb{R}^N}d\lambda\;|\det M(v,Q,C)|\,e^{-\alpha C^2-\beta\lambda^2+i\lambda_a(v_a-(Q_{abc}+C_{abc})v_bv_c)}.\qquad(7)$$

The part $|\det M(v,Q,C)|$ in Eq. (7) needs a special care, because taking an absolute value is not an analytic function. In Sect. 3, we will consider the case that we ignore taking the absolute value. This makes the problem easier and treatable by introducing only a pair of fermions, but is still nontrivial and interesting. In Sect. 4, we will fully treat Eq. (7) by introducing both bosons and fermions.

3. Signed distributions

3.1. *Quantum field theory expression*

The quantity we will compute in this section is defined by ignoring taking the absolute value in Eq. (7):

$$\rho^{\text{signed}}(v,Q,\beta)=\frac{1}{(2\pi)^NA}\int_{\mathbb{R}^{\#C}}dC\int_{\mathbb{R}^{\mathbb{N}}}d\lambda\,\det M(v,Q,C)\,e^{-\alpha C^2-\beta\lambda^2+i\lambda_a(v_a-(Q_{abc}+C_{abc})v_bv_c)}.\qquad(8)$$

Following backward the derivation in Sect. 2, the distribution corresponds to a "signed" distribution,

$$\rho^{\text{signed}}(v,Q,C,\eta)=\sum_{i=1}^{\#\text{sol}(Q,C,\eta)}\text{sign}\left(\det M(v^i,Q,C)\right)\prod_{a=1}^{N}\delta\left(v_a-v_a^i\right),\qquad(9)$$

which has an extra sign of $\det M(v^i,Q,C)$ dependent on each solution v^i, compared with Eq. (3). Note that the quantity (8) is a generalization of the signed distribution computed in Ref. [24] to the case with backgrounds and deviations. Though the quantity has no clear connections to Eq. (7), it provides a simpler playground, and we will obtain an exact final expression with the confluent hypergeometric functions of the second kind (or hermite polynomials).

The determinant factor in Eq. (8) can easily be rewritten in a quantum field theoretical form by introducing a fermion pair, $\bar\psi_a$, ψ_a $(a=1,2,\cdots,N)$; $\det M=\int d\bar\psi d\psi\,e^{\bar\psi M\psi}$ [31]. This tech-

[5] Explicitly, $\#C=N(N+1)(N+2)/6$.

nique to incorporate determinants in quantum field theories is common in treating disordered systems in statistical physics.[6] Then Eq. (8) can be rewritten as

$$\rho^{\text{signed}}(v, Q, \beta) = \frac{1}{(2\pi)^N A} \int_{\mathbb{R}^{\#C}} dC \int_{\mathbb{R}^N} d\lambda \int d\bar{\psi} d\psi \, e^{S_{\text{bare}}^{\text{signed}}}, \tag{10}$$

where

$$S_{\text{bare}}^{\text{signed}} = -\alpha C^2 - \beta\lambda^2 + i\lambda_a(v_a - (Q_{abc} + C_{abc})v_b v_c) + \bar{\psi}_a (\delta_{ab} - 2(Q_{abc} + C_{abc})v_c)\, \psi_b. \tag{11}$$

Since C and λ appear quadratically at the highest in Eq. (11), they can be integrated out by Gaussian integrations. We will first integrate over C and then over λ. Though the integrations are straightforward, the actual computation is a little cumbersome, because of the anticommuting nature of the fermions and the necessity of symmetrization for the indices of C_{abc}. However, we can take a shortcut by taking some results from Ref. [24], where there are no Q or η. Now, new terms in $S_{\text{bare}}^{\text{signed}}$ compared to Ref. [24] are those depending on Q and β, and are explicitly given by

$$S_{\text{new}}^{\text{signed}} = -\beta\lambda^2 - i\lambda_a Q_{abc} v_b v_c - 2Q_{abc}\bar{\psi}_a\psi_b v_c. \tag{12}$$

Since the new terms do not contain C, the integration over C proceeds in the same way as in Ref. [24]. This integration cancels the overall factor A^{-1} in Eq. (10), and also generates various terms being added to the action. Collecting the terms depending on λ among the generated ones, $i\lambda_a v_a$ in Eq. (11), and the terms depending on λ in Eq. (12), we obtain the λ-dependent part of the action as

$$S_\lambda^{\text{signed}} = -\frac{v^4}{12\alpha} B_{ab}\lambda_a\lambda_b + i\lambda_a \left(v_a + D_a^{\text{signed}} - D_a^Q\right), \tag{13}$$

where $D_a^Q = Q_{abc}v_b v_c$, and D^{signed} can be taken from Ref. [24],[7]

$$D_a^{\text{signed}} = \frac{1}{3\alpha}\left(\bar{\psi}_a\,\psi\cdot v\, v^2 + \bar{\psi}\cdot v\,\psi_a\, v^2 + \bar{\psi}\cdot v\,\psi\cdot v\, v_a\right). \tag{14}$$

Here we very frequently use an abusive notation $v^p := |v|^p$ for simplicity throughout this paper, since whether v means vector or scalar quantities is always obvious from contexts. The matrix B is given by

$$B = 3\left(1 + \frac{4\alpha\beta}{v^4}\right) I_\parallel + \left(1 + \frac{12\alpha\beta}{v^4}\right) I_\perp, \tag{15}$$

where $I_\parallel$ and $I_\perp$ are the projection matrices to the parallel and the transverse subspaces against v: $I_{\parallel ab} = v_a v_b/v^2$, $I_{\perp ab} = \delta_{ab} - v_a v_b/v^2$. Then the integration over λ with the action (13) generates an action,

$$\begin{aligned}\delta S_\lambda^{\text{signed}} = &-\frac{N}{2}\log\frac{v^4}{12\pi\alpha} - \frac{1}{2}\log\det B - \frac{3\alpha}{v^4}\left(\left(v_a + D_a^{\text{signed}}\right) B_{ab}^{-1}\left(v_b + D_b^{\text{signed}}\right)\right. \\ &\left. - 2\left(v_a + D_a^{\text{signed}}\right) B_{ab}^{-1} D_b^Q + D_a^Q B_{ab}^{-1} D_b^Q\right),\end{aligned} \tag{16}$$

where the inverse of B is given by

$$B^{-1} = \frac{b_\parallel}{3} I_\parallel + b_\perp I_\perp \tag{17}$$

[6] See, e.g. Ref. [32] and references therein.

[7] $v_a + D_a^{\text{signed}}$ corresponds to D_a of Ref. [24].

with

$$b_\parallel = \frac{v^4}{v^4 + 4\alpha\beta},$$

$$b_\perp = \frac{v^4}{v^4 + 12\alpha\beta}. \tag{18}$$

When we consider the case with $Q = \beta = 0$, the distribution (10) should agree with the previous result of Ref. [24]. Therefore, it is enough for us to compute the additional part which appears only when $Q \neq 0$ or $\beta \neq 0$. By subtracting $\delta S_\lambda^{\text{signed}}$ for $Q = \beta = 0$ in Eq. (16) and using Eq. (17), we obtain

$$\begin{aligned}\delta S_\lambda^{\text{signed}} - \delta S_\lambda^{\text{signed}}(Q = \beta = 0) = \frac{1}{2}\log b_\parallel + \frac{N-1}{2}\log b_\perp - \frac{3\alpha}{v^4}\Bigg[\frac{b_\parallel - 1}{3}\left(v + D_\parallel^{\text{signed}}\right)^2 \\ + (b_\perp - 1)\, D_\perp^{\text{signed}} \cdot D_\perp^{\text{signed}} - \frac{2b_\parallel}{3}\left(v + D_\parallel^{\text{signed}}\right) D_\parallel^Q \\ - 2b_\perp D_\perp^{\text{signed}} \cdot D_\perp^Q + \frac{b_\parallel}{3}\left(D_\parallel^Q\right)^2 + b_\perp D_\perp^Q \cdot D_\perp^Q\Bigg],\end{aligned} \tag{19}$$

where $D_\parallel^{\text{signed}} = v \cdot D^{\text{signed}}/|v|$, $D_\perp^{\text{signed}} = I_\perp D^{\text{signed}}$, $D_\parallel^Q = v \cdot D^Q/|v|$, $D_\perp^Q = I_\perp D^Q$.

The previous result in Ref. [24] is given by

$$\rho^{\text{signed}}(v, Q = 0, \beta = 0) = 3^{\frac{N-1}{2}} \pi^{-\frac{N}{2}} \alpha^{\frac{N}{2}} \int d\bar\psi d\psi\, e^{S_{\bar\psi\psi}}, \tag{20}$$

where

$$S_{\bar\psi\psi} = -\frac{\alpha}{v^2} - 2N\log v + \bar\psi_\perp \cdot \psi_\perp - \bar\psi_\parallel \psi_\parallel - \frac{v^2}{6\alpha}\left(\bar\psi_\perp \cdot \psi_\perp\right)^2 \tag{21}$$

with $\psi_\parallel = v \cdot \psi/|v|, \psi_\perp = I_\perp \psi$, etc. Adding Eq. (19) and the last term in Eq. (12) to Eq. (21) and doing some straightforward computations, we finally obtain

$$\begin{aligned}\rho^{\text{signed}}(v, Q, \beta) = 3^{\frac{N-1}{2}} \pi^{-\frac{N}{2}} \alpha^{\frac{N}{2}} (v^4 + 4\alpha\beta)^{-\frac{1}{2}} (v^4 + 12\alpha\beta)^{-\frac{N-1}{2}} \exp\left[-\frac{\alpha v^2}{v^4 + 4\alpha\beta}\right] \\ \cdot \exp\left[\frac{2\alpha b_\parallel v D_\parallel^Q - \alpha b_\parallel \left(D_\parallel^Q\right)^2 - 3\alpha b_\perp D_\perp^Q \cdot D_\perp^Q}{v^4}\right] \int d\bar\psi d\psi\, e^{S^{\text{signed}}},\end{aligned} \tag{22}$$

where

$$\begin{aligned}S^{\text{signed}} = \left(-2b_\parallel + 1 + \frac{2b_\parallel D_\parallel^Q}{v}\right)\bar\psi_\parallel \psi_\parallel + \frac{2b_\perp}{v} D_\perp^Q \cdot \left(\bar\psi_\perp \psi_\parallel + \bar\psi_\parallel \psi_\perp\right) + \bar\psi_\perp \cdot \psi_\perp \\ - 2Q_{abc}\bar\psi_a \psi_b v_c + \frac{2v^2(b_\perp - 1)}{3\alpha}\bar\psi_\parallel \psi_\parallel \bar\psi_\perp \cdot \psi_\perp - \frac{v^2}{6\alpha}\left(\bar\psi_\perp \cdot \psi_\perp\right)^2.\end{aligned} \tag{23}$$

Some details of the derivation are explained in Appendix A.

3.2. *Rank-one Q*

To study the formula Eq. (22) with Eq. (23) more explicitly, let us consider the case that Q is a rank-one tensor,

$$Q_{abc} = q\, n_a n_b n_c, \tag{24}$$

where q is real and n is a normalized real vector ($|n| = 1$). This is a setup called a spiked tensor [27].

In the general situation, the vector n is a linear combination of v and another vector n_1, which is a normalized vector transverse to v (namely, $v \cdot n_1 = 0,\ |n_1| = 1$). Then the transverse subspace to v can further be divided into the subspace parallel to n_1 and the $N-2$-dimensional subspace transverse to both v and n_1. We denote the projector to the latter by $I_{\perp_2}$. Then the transverse fermions, $\bar\psi_\perp, \psi_\perp$, can further be decomposed into $\bar\psi_{\perp_1} = n_1 \cdot \bar\psi$ and $\bar\psi_{\perp_2} = I_{\perp_2}\bar\psi$ and similarly for $\psi_\perp$. Note that $\bar\psi_\perp \cdot \psi_\perp = \bar\psi_{\perp_1}\psi_{\perp_1} + \bar\psi_{\perp_2}\cdot\psi_{\perp_2}$, etc.

For Eq. (24), $D_\parallel^Q = qv^2 n_\parallel^3,\ D_\perp^Q = qv^2 n_\parallel^2 n_\perp n_1$, where $n_\parallel = v\cdot n/|v|, n_\perp = n_1 \cdot n$. We also notice

$$Q_{abc}v_c\bar\psi_a\psi_b = qn_an_bn_cv_a\psi_b\psi_c = qvn_\parallel^3\bar\psi_\parallel\psi_\parallel + qvn_\parallel^2 n_\perp(\bar\psi_\parallel\psi_{\perp_1} + \bar\psi_{\perp_1}\psi_\parallel) + qvn_\parallel n_\perp^2\bar\psi_{\perp_1}\psi_{\perp_1}. \tag{25}$$

Putting these into Eqs. (22) and (23), we obtain

$$\rho_{\text{spiked}}^{\text{signed}}(v,n,q,\beta) = 3^{\frac{N-1}{2}}\pi^{-\frac{N}{2}}\alpha^{\frac{N}{2}}(v^4+4\alpha\beta)^{-\frac{1}{2}}(v^4+12\alpha\beta)^{-\frac{N-1}{2}} \\ \cdot\ \exp\left[\frac{-\alpha v^2 + 2\alpha qv^3n_\parallel^3 - \alpha q^2v^4n_\parallel^6}{v^4+4\alpha\beta} - \frac{3\alpha q^2v^4n_\parallel^4n_\perp^2}{v^4+12\alpha\beta}\right]\int d\bar\psi d\psi\, e^{S_{\text{spiked}}^{\text{signed}}}, \tag{26}$$

where

$$S_{\text{spiked}}^{\text{signed}} = -\left(\frac{v^4-4\alpha\beta}{v^4+4\alpha\beta} + \frac{8\alpha\beta qvn_\parallel^3}{v^4+4\alpha\beta}\right)\bar\psi_\parallel\psi_\parallel - \frac{24\alpha\beta qvn_\parallel^2n_\perp}{v^4+12\alpha\beta}\left(\bar\psi_\parallel\psi_{\perp_1} + \bar\psi_{\perp_1}\psi_\parallel\right) \\ +\ \left(1-2qvn_\parallel n_\perp^2\right)\bar\psi_{\perp_1}\psi_{\perp_1} + \bar\psi_{\perp_2}\cdot\psi_{\perp_2} - \frac{8\beta v^2}{v^4+12\alpha\beta}\bar\psi_\parallel\psi_\parallel\left(\bar\psi_{\perp_1}\psi_{\perp_1} + \bar\psi_{\perp_2}\cdot\psi_{\perp_2}\right) \\ -\ \frac{v^2}{6\alpha}\left(\bar\psi_{\perp_1}\psi_{\perp_1} + \bar\psi_{\perp_2}\cdot\psi_{\perp_2}\right)^2. \tag{27}$$

It is not difficult to compute explicitly the fermion integration in Eq. (26). As is shown in Appendix B, we obtain

$$\int d\bar\psi d\psi\, e^{S_{\text{spiked}}^{\text{signed}}} = 2^{N-6}(-d_2)^{\frac{N-5}{2}}\Bigg[-8d_2(-b_2^2+d_1+b_3(b_1+d_1)+2b_1d_2)\,U\left(\frac{3-N}{2},\frac{3}{2},-\frac{1}{4d_2}\right) \\ + 2(N-3)(b_3d_1+2b_1d_2+6d_1d_2)\,U\left(\frac{5-N}{2},\frac{5}{2},-\frac{1}{4d_2}\right) \\ - d_1(N-3)(N-5)\,U\left(\frac{7-N}{2},\frac{7}{2},-\frac{1}{4d_2}\right)\Bigg], \tag{28}$$

where U denotes the confluent hypergeometric function of the second kind, and b_i, d_i are the coefficients of the terms in Eq. (27):

$$b_1 = -\left(\frac{v^4-4\alpha\beta}{v^4+4\alpha\beta} + \frac{8\alpha\beta qvn_\parallel^3}{v^4+4\alpha\beta}\right),\ b_2 = -\frac{24\alpha\beta qvn_\parallel^2n_\perp}{v^4+12\alpha\beta},\ b_3 = 1-2qvn_\parallel n_\perp^2, \\ d_1 = -\frac{8\beta v^2}{v^4+12\alpha\beta},\ d_2 = -\frac{v^2}{6\alpha}. \tag{29}$$

The result (26) with Eq. (28) gives the exact expression of the signed distribution.

4. Distributions

4.1. *Quantum field theory expression*

In this subsection we obtain the quantum field theoretical expressions of the (authentic) distribution by considering the determinant factor $|\det M|$ as it is. We take the same procedure as was employed in Ref. [26]. We first introduce bosons and fermions to rewrite $|\det M|$:

$$
\begin{aligned}
|\det M| &= \lim_{\epsilon\to+0} \frac{\det(M^2+\epsilon I)}{\sqrt{\det(M^2+\epsilon I)}} \\
&= (-\pi)^{-N} \int d\bar{\psi} d\psi d\bar{\varphi} d\varphi d\phi d\sigma \, e^{-\sigma^2 - 2i\sigma M\phi - \epsilon\phi^2 - \bar{\varphi}\varphi - \bar{\psi}M\varphi - \bar{\varphi}M\psi + \epsilon\bar{\psi}\psi}, \qquad (30)
\end{aligned}
$$

where I is an identity matrix of N-by-N, ϕ_a, σ_a are real bosons, $\bar{\psi}_a, \psi_a, \bar{\varphi}_a, \varphi_a$ are fermions, and $\bar{\psi}\psi = \bar{\psi}_a\psi_a$, etc. Here we have introduced a positive infinitesimal parameter ϵ to regularize the expression, since M may have zero eigenvalues. As in the second line, writing the limit is suppressed to simplify the notation hereafter, assuming implicitly taking this limit at ends of computations. In fact, the limit turns out to be straightforward in all the computations of this paper. We have introduced two sets of bosons and fermions to make the exponent linear in C (M contains C linearly) for later convenience of the integration over C. By performing similar processes as in Sect. 3, we obtain

$$
\rho(v, Q, \beta) = \frac{(-1)^N}{2^N \pi^{2N} A} \int dC d\lambda d\bar{\psi} d\psi d\bar{\varphi} d\varphi d\phi d\sigma \, e^{S_{\text{bare}}}, \qquad (31)
$$

where

$$
\begin{aligned}
S_{\text{bare}} = &-\alpha C^2 - \beta\lambda^2 + i\lambda_a(v_a - (C_{abc} + Q_{abc})v_b v_c) \\
&- \sigma^2 - 2i\sigma_a \left(\delta_{ab} - 2(Q_{abc} + C_{abc})v_c\right)\phi_b - \epsilon\phi^2 \\
&- \bar{\varphi}\varphi - \bar{\psi}_a \left(\delta_{ab} - 2(Q_{abc} + C_{abc})v_c\right)\varphi_b - \bar{\varphi}_a \left(\delta_{ab} - 2(Q_{abc} + C_{abc})v_c\right)\psi_b + \epsilon\bar{\psi}\psi. \qquad (32)
\end{aligned}
$$

As in Sect. 3, there are no new terms depending on C compared with the previous case for $Q = \beta = 0$ in Ref. [26], and therefore the integration over C can be performed as in the previous computation there. Then we obtain a similar form of the action for λ as in Sect. 3:

$$
S_\lambda = -\frac{v^4}{12\alpha}\lambda_a B_{ab}\lambda_b + i\lambda_a\left(v_a - D_a - D_a^Q\right), \qquad (33)
$$

where B, D^Q are already defined in Eq. (15) and below Eq. (13), respectively. Here D can be taken from Ref. [26]:[8]

$$
D_a = \frac{v^3}{3\alpha}\Big[(\bar{\psi}_\parallel\varphi_\parallel + \bar{\varphi}_\parallel\psi_\parallel)\hat{v}_a + \bar{\psi}_a\varphi_\parallel + \bar{\psi}_\parallel\varphi_a + \bar{\varphi}_a\psi_\parallel + \bar{\varphi}_\parallel\psi_a + 2i\left(\hat{v}_a\sigma_\parallel\phi_\parallel + \sigma_a\phi_\parallel + \sigma_\parallel\phi_a\right)\Big], \qquad (34)
$$

where $\hat{v}_a = v_a/|v|$. Comparing Eq. (33) with Eq. (13), the change is to replace D^{signed} with $-D$. By using Eq. (19) with this replacement and adding the Q-dependent but λ-independent terms

[8] Here D is the sum $D + \tilde{D}$ of Ref. [26].

in Eq. (32), we obtain

$$\rho(v, Q, \beta) = 3^{\frac{N-1}{2}} \pi^{-\frac{3N}{2}} \alpha^{\frac{N}{2}} (v^4 + 4\alpha\beta)^{-\frac{1}{2}} (v^4 + 12\alpha\beta)^{-\frac{N-1}{2}} \exp\left[-\frac{\alpha v^2}{v^4 + 4\alpha\beta}\right]$$
$$\cdot \exp\left[\frac{2\alpha b_\parallel v D_\parallel^Q - \alpha b_\parallel \left(D_\parallel^Q\right)^2 - 3\alpha b_\perp D_\perp^Q \cdot D_\perp^Q}{v^4}\right] Z, \tag{35}$$

where Z is a partition function of a quantum field theory,

$$Z = (-1)^N \int d\bar{\psi} \cdots d\sigma \, e^{S_0 + S_{Q,\beta}}. \tag{36}$$

Here S_0 is the former result in Ref. [26] corresponding to $Q = \beta = 0$, which is explicitly given in Appendix C, and

$$S_{Q,\beta} = \frac{2\alpha(b_\parallel - 1)v - 2\alpha b_\parallel D_\parallel^Q}{v^4} D_\parallel - \frac{6\alpha b_\perp}{v^4} D_\perp \cdot D_\perp^Q + 2Q_{abc} v_c \left(\bar{\psi}_a \varphi_b + \bar{\varphi}_a \psi_b + 2i\sigma_a \phi_b\right)$$
$$- \frac{\alpha(b_\parallel - 1)}{v^4} D_\parallel^2 - \frac{3\alpha(b_\perp - 1)}{v^4} D_\perp \cdot D_\perp, \tag{37}$$

where $D_\parallel = v \cdot D/|v|, D_\perp = I_\perp D$. Note that the first three terms are some corrections to the kinetic terms, and the latter to the four-interaction terms. As for $D_\parallel$ and $D_\perp$, we have more explicit expressions from Eq. (34),

$$D_\parallel = \frac{v^3}{\alpha} \left(\bar{\psi}_\parallel \varphi_\parallel + \bar{\varphi}_\parallel \psi_\parallel + 2i\sigma_\parallel \phi_\parallel\right),$$
$$D_\perp = \frac{v^3}{3\alpha} \left(\bar{\psi}_\perp \varphi_\parallel + \bar{\psi}_\parallel \varphi_\perp + \bar{\varphi}_\perp \psi_\parallel + \bar{\varphi}_\parallel \psi_\perp + 2i(\sigma_\parallel \phi_\perp + \sigma_\perp \phi_\parallel)\right). \tag{38}$$

The four-interaction terms in Eq. (37) have the form of self-products. One can make them quadratic by using the formula $\frac{1}{\sqrt{\pi}} \int_{\mathbb{R}} dg \, e^{-g^2 + 2Ag} = e^{A^2}$. The result is

$$Z = (-1)^N \pi^{-\frac{N}{2}} \int dg_\parallel dg_\perp d\bar{\psi} \cdots d\sigma \, e^{S_0 + S_{Q,\beta,g}}, \tag{39}$$

where $g_\parallel$ is 1-dimensional, $g_\perp$ is $N-1$-dimensional, and[9]

$$S_{Q,\beta,g} = -g_\parallel^2 - g_\perp^2 + \left(\frac{2\alpha(b_\parallel - 1)v - 2\alpha b_\parallel D_\parallel^Q}{v^4} + \frac{2\sqrt{\alpha(1 - b_\parallel)}}{v^2} g_\parallel\right) D_\parallel - \frac{6\alpha b_\perp}{v^4} D_\perp \cdot D_\perp^Q$$
$$+ \frac{2\sqrt{3\alpha(1 - b_\perp)}}{v^2} D_\perp \cdot g_\perp + 2Q_{abc} v_c \left(\bar{\psi}_a \varphi_b + \bar{\varphi}_a \psi_b + 2i\sigma_a \phi_b\right), \tag{40}$$

which contains only quadratic terms of the fields.

4.2. *Rank-one Q*

In this subsection we consider the rank-one tensor Q in Eq. (24) to perform explicitly the integration over the fields in Eq. (35).

[9]Note that $b_\parallel, b_\perp < 1$.

4.2.1. *A general formula.* By putting Eq. (24) into Eq. (35), one obtains

$$\rho(v, Q, \beta) = 3^{\frac{N-1}{2}} \pi^{-\frac{3N}{2}} \alpha^{\frac{N}{2}} (v^4 + 4\alpha\beta)^{-\frac{1}{2}} (v^4 + 12\alpha\beta)^{-\frac{N-1}{2}} \exp\left[-\frac{\alpha v^2}{v^4 + 4\alpha\beta}\right]$$
$$\cdot \exp\left[\frac{2\alpha q v^3 n_\parallel^3 - \alpha q^2 v^4 n_\parallel^6}{v^4 + 4\alpha\beta} - \frac{3\alpha q^2 v^4 n_\parallel^4 n_\perp^2}{v^4 + 12\alpha\beta}\right] Z, \tag{41}$$

where the partition function Z can be computed either by Eq. (36) with Eq. (37) or by Eq. (39) with Eq. (40).

Let us first put Eq. (24) into Eq. (37). After a lengthy but straightforward computation using the same decomposition as in Sect. 3.2, we get

$$\begin{aligned}
S_{q,n,\beta} &:= S_{Q=qnnn,\beta} \\
&= 2(qvn_\parallel^3 - 1)(1 - b_\parallel)\left(\bar{\psi}_\parallel \varphi_\parallel + \bar{\varphi}_\parallel \psi_\parallel + 2i\sigma_\parallel \phi_\parallel\right) \\
&\quad + 2qvn_\parallel^2 n_\perp (1 - b_\perp)\left(\bar{\psi}_{\perp_1}\varphi_\parallel + \bar{\psi}_\parallel \varphi_{\perp_1} + \bar{\varphi}_{\perp_1}\psi_\parallel + \bar{\varphi}_\parallel \psi_{\perp_1} + 2i(\sigma_\parallel \phi_{\perp_1} + \sigma_{\perp_1}\phi_\parallel)\right) \\
&\quad + 2qvn_\parallel n_\perp^2 \left(\bar{\psi}_{\perp_1}\varphi_{\perp_1} + \bar{\varphi}_{\perp_1}\psi_{\perp_1} + 2i\sigma_{\perp_1}\phi_{\perp_1}\right) \\
&\quad + \frac{8\beta v^2}{v^4 + 4\alpha\beta}\left(-\bar{\psi}_\parallel \psi_\parallel \bar{\varphi}_\parallel \varphi_\parallel + 2i(\bar{\psi}_\parallel \varphi_\parallel + \bar{\varphi}_\parallel \psi_\parallel)\sigma_\parallel \phi_\parallel - 2{\sigma_\parallel}^2 {\phi_\parallel}^2\right) \\
&\quad + \frac{8\beta v^2}{v^4 + 12\alpha\beta}\Big(\bar{\psi}_\perp \cdot \bar{\varphi}_\perp \psi_\parallel \varphi_\parallel + \psi_\perp \cdot \varphi_\perp \bar{\psi}_\parallel \bar{\varphi}_\parallel - \bar{\psi}_\perp \cdot \psi_\perp \bar{\varphi}_\parallel \varphi_\parallel - \bar{\psi}_\perp \cdot \varphi_\perp \bar{\psi}_\parallel \varphi_\parallel \\
&\quad - \bar{\varphi}_\perp \cdot \varphi_\perp \bar{\psi}_\parallel \psi_\parallel - \bar{\varphi}_\perp \cdot \psi_\perp \bar{\varphi}_\parallel \psi_\parallel \\
&\quad + 2i\left(\bar{\psi}_\perp \varphi_\parallel + \bar{\psi}_\parallel \varphi_\perp + \bar{\varphi}_\perp \psi_\parallel + \bar{\varphi}_\parallel \psi_\perp\right) \cdot (\sigma_\parallel \phi_\perp + \sigma_\perp \phi_\parallel) \\
&\quad - 2\left({\sigma_\parallel}^2 \phi_\perp \cdot \phi_\perp + {\phi_\parallel}^2 \sigma_\perp \cdot \sigma_\perp + 2\sigma_\parallel \phi_\parallel \phi_\perp \cdot \sigma_\perp\right)\Big).
\end{aligned} \tag{42}$$

As for Eq. (40), we obtain

$$\begin{aligned}
S_{q,n,\beta,g} &:= S_{Q=qnnn,\beta,g} \\
&= -g_\parallel^2 - g_\perp^2 + 2\left((qvn_\parallel^3 - 1)(1 - b_\parallel) + v\sqrt{\frac{1 - b_\parallel}{\alpha}} g_\parallel\right)\left(\bar{\psi}_\parallel \varphi_\parallel + \bar{\varphi}_\parallel \psi_\parallel + 2i\sigma_\parallel \phi_\parallel\right) \\
&\quad + \left(2qvn_\parallel^2 n_\perp (1 - b_\perp)\right)\left(\bar{\psi}_{\perp_1}\varphi_\parallel + \bar{\psi}_\parallel \varphi_{\perp_1} + \bar{\varphi}_{\perp_1}\psi_\parallel + \bar{\varphi}_\parallel \psi_{\perp_1} + 2i(\sigma_\parallel \phi_{\perp_1} + \sigma_{\perp_1}\phi_\parallel)\right) \\
&\quad + 2qvn_\parallel n_\perp^2 \left(\bar{\psi}_{\perp_1}\varphi_{\perp_1} + \bar{\varphi}_{\perp_1}\psi_{\perp_1} + 2i\sigma_{\perp_1}\phi_{\perp_1}\right) \\
&\quad + 2v\sqrt{\frac{1 - b_\perp}{3\alpha}} g_\perp \cdot \left(\bar{\psi}_\perp \varphi_\parallel + \bar{\psi}_\parallel \varphi_\perp + \bar{\varphi}_\perp \psi_\parallel + \bar{\varphi}_\parallel \psi_\perp + 2i(\sigma_\parallel \phi_\perp + \sigma_\perp \phi_\parallel)\right).
\end{aligned} \tag{43}$$

In the following subsections, we will consider $N = 1$, $N = 2$, and large-N cases.

4.2.2. *N = 1.* In this case we ignore all the transverse components, and also set $n_\parallel = 1$. By putting these into Eqs. (35), (39), (43), and (C2), and doing some straightforward computations, we obtain

$$\rho(v,q,\beta)=\pi^{-1}\alpha^{\frac{1}{2}}(v^4+4\alpha\beta)^{-\frac{1}{2}}\exp\left[\frac{-\alpha v^2+2\alpha q v^3-\alpha q^2 v^4}{v^4+4\alpha\beta}\right]\left(\sqrt{\pi}\,a\,\mathrm{Erf}\left(\frac{a}{b}\right)+b\,e^{-\frac{a^2}{b^2}}\right),\tag{44}$$

where

$$a=1+2(qv-1)(1-b_\parallel),$$
$$b=2v\sqrt{\frac{(1-b_\parallel)}{\alpha}}.\tag{45}$$

The details of the derivation are given in Appendix D.

4.2.3. *N = 2.* In this case the transverse direction is exhausted by one dimension, namely, $\perp = \perp_1$, and $\perp_2$ is null. A special fact about this case is that the four-interaction terms in Eq. (C2) have the form of a square:

$$V_F+V_B+V_{BF}=\frac{v^2}{3\alpha}\left(\bar\psi_{\perp_1}\varphi_{\perp_1}+\bar\varphi_{\perp_1}\psi_{\perp_1}+2i\sigma_{\perp_1}\phi_{\perp_1}\right)^2.\tag{46}$$

Therefore, we can rewrite this part of the action as

$$e^{V_F+V_B+V_{BF}}=\frac{1}{\sqrt{\pi}}\int dg\,e^{-g^2+2vg\left(\bar\psi_{\perp_1}\varphi_{\perp_1}+\bar\varphi_{\perp_1}\psi_{\perp_1}+2i\sigma_{\perp_1}\phi_{\perp_1}\right)/\sqrt{3\alpha}},\tag{47}$$

whose exponent contains only quadratic terms of the fields. Using this for Eqs. (39), (43), and (C2), we obtain

$$Z_{N=2}=\pi^{-\frac{3}{2}}\int dg_1dg_2dg_3\int d\bar\psi\cdots d\sigma\,e^{-g_1^2-g_2^2-g_3^2+K_{\parallel\perp_1}},\tag{48}$$

where

$$\begin{aligned}K_{\parallel\perp_1}=&-\bar\varphi_\parallel\varphi_\parallel+\epsilon\bar\psi_\parallel\psi_\parallel-{\sigma_\parallel}^2-\epsilon{\phi_\parallel}^2-\bar\varphi_{\perp_1}\varphi_{\perp_1}+\epsilon\bar\psi_{\perp_1}\psi_{\perp_1}-{\sigma_{\perp_1}}^2-\epsilon{\phi_{\perp_1}}^2\\&+a_1\left(\bar\psi_\parallel\varphi_\parallel+\bar\varphi_\parallel\psi_\parallel+2i\sigma_\parallel\phi_\parallel\right)\\&+a_2\left(\bar\psi_\parallel\varphi_{\perp_1}+\bar\psi_{\perp_1}\varphi_\parallel+\bar\varphi_\parallel\psi_{\perp_1}+\bar\varphi_{\perp_1}\psi_\parallel+2i\left(\sigma_\parallel\phi_{\perp_1}+\sigma_{\perp_1}\phi_\parallel\right)\right)\\&+a_3\left(\bar\psi_{\perp_1}\varphi_{\perp_1}+\bar\varphi_{\perp_1}\psi_{\perp_1}+2i\sigma_{\perp_1}\phi_{\perp_1}\right)\end{aligned}\tag{49}$$

with

$$a_1=2b_\parallel-1+2qv(1-b_\parallel)n_\parallel^3+2v\sqrt{\frac{1-b_\parallel}{\alpha}}g_1,$$
$$a_2=2qv(1-b_\perp)n_\parallel^2n_\perp+2v\sqrt{\frac{1-b_\perp}{3\alpha}}g_2,$$
$$a_3=-1+2qvn_\parallel n_\perp^2+2v\sqrt{\frac{1}{3\alpha}}g_3.\tag{50}$$

Then the integration (48) over the fields generates a square root of a determinant, and we obtain

$$Z_{N=2}=\sqrt{\pi}\int dg_1dg_2dg_3\,e^{-g_1^2-g_2^2-g_3^2}\left|a_2^2-a_1a_3\right|.\tag{51}$$

4.2.4. *Large N.* For $N>2$ we will not obtain exact expressions of the distributions. We will rather obtain an expression which is a good approximation for large N. For large N the degrees of freedom carried by the $\perp_2$ fields will dominate over those of the $\|\perp_1$ fields, since the former is $(N-2)$-dimensional, whereas the latter is 2-dimensional. Therefore, the dynamics of the $\perp_2$ fields can well be determined by themselves with little effects from the $\|\perp_1$ fields, which may be ignored in the large-N limit. Then the dynamics of the $\|\perp_1$ fields may be computed in the backgrounds of the $\perp_2$ fields, which can well be approximated by their classical values because of their large number of degrees of freedom for large N.

More precisely, our approximation is given by

$$Z = Z_{\perp_2} Z_{\|\perp_1}(R). \tag{52}$$

Here $Z_{\perp_2}$ is the partition function determined solely by the $\perp_2$ fields,

$$Z_{\perp_2} = (-1)^{N-2} \int d\bar{\psi}_{\perp_2} \cdots d\sigma_{\perp_2}\, e^{S_{\perp_2}}, \tag{53}$$

where $S_{\perp_2}$ is the collection of the terms which contain only the $\perp_2$ fields in Eq. (C1) with Eq. (C2).[10] The computation of the partition function $Z_{\perp_2}$ is the same as that in the previous paper [26], because $S_{\perp_2}$ has the same form as the action of the transverse directions there.[11]

$Z_{\|\perp_1}(R)$ is the partition function of the $\|\perp_1$ fields in the background of the $\perp_2$ fields,

$$Z_{\|\perp_1}(R) = \int d\bar{\psi}_{\|} \cdots d\sigma_{\perp_1} e^{S_{\|\perp_1}(R)}, \tag{54}$$

where R denotes the classical backgrounds of the $\perp_2$ fields, as will be explained below in more detail. Here the action $S_{\|\perp_1}(R)$ is composed of all the terms which contain the $\|\perp_1$ fields in Eqs. (42) and (C1). Part of the terms in $S_{\|\perp_1}(R)$ contain the $\perp_2$ fields as well. For large N these $\perp_2$ fields may well be approximated by their classical values because of the large degrees of freedom of the $\perp_2$ fields. For instance, we perform replacements,

$$\bar{\psi}_{\perp_2} \cdot \varphi_{\perp_2} \bar{\psi}_{\|} \varphi_{\|} \rightarrow \langle \bar{\psi}_{\perp_2} \cdot \varphi_{\perp_2} \rangle \bar{\psi}_{\|} \varphi_{\|}, \tag{55}$$

where $\langle \cdot \rangle$ denotes an expectation value. By doing such replacements we obtain $S_{\|\perp_1}(R)$, whose dynamical fields are only the $\|\perp_1$ fields.

Obtaining the explicit form of $S_{\|\perp_1}(R)$ proceeds as follows. The quadratic and quartic terms of the $\|\perp_1$ fields can be processed in the same manner as are performed for $N=2$ in Sect. 4.2.3, and we obtain $K_{\|\perp_1}$ in Eq. (49) with Eq. (50). Then the four-interaction terms between the $\|\perp_1$ fields and the $\perp_2$ fields, where the latter are replaced by their expectation values like in Eq. (55), generate some quadratic terms of the former, which are explicitly given in Eq. (E7) of Appendix E. Thus we have

$$S_{\|\perp_1}(R) = K_{\|\perp_1} + V_{\|\perp_1,\perp_2}(R), \tag{56}$$

whose terms are all quadratic in the $\|\perp_1$ fields. Then the computation of the partition function (54) is just a computation of a determinant, and we obtain

$$Z_{\|\perp_1}(R) = \sqrt{\pi} \int dg_1 dg_2 dg_3\, e^{-g_1^2 - g_2^2 - g_3^2} \sqrt{\det H}, \tag{57}$$

[10] For instance, we include $\bar{\psi}_{\perp_2} \cdot \psi_{\perp_2} \bar{\varphi}_{\perp_2} \cdot \varphi_{\perp_2}$ but ignore $\bar{\psi}_{\perp_2} \cdot \psi_{\perp_2} \bar{\varphi}_{\perp_1} \varphi_{\perp_1}$, $\bar{\psi}_{\perp_2} \cdot \psi_{\perp_2} \bar{\varphi}_{\|} \varphi_{\|}$, etc., because of the reason mentioned in the first paragraph. The ignored terms will be considered in $Z_{\|\perp_1}$.

[11] But note the difference of the dimensions of $\perp_2$ here and $\perp$ in Ref. [26], where the former is $N-2$, whereas the latter is $N-1$. Therefore, when we take a result from Ref. [26], we have to deduct N by one.

where H is given by

$$H = \begin{pmatrix} \epsilon - A_1 R_{22} & a_1 - A_1 R_{12} & 0 & a_2 \\ a_1 - A_1 R_{12} & -1 - A_1 R_{11} & a_2 & 0 \\ 0 & a_2 & \epsilon - A_2 R_{22} & a_3 - A_2 R_{12} \\ a_2 & 0 & a_3 - A_2 R_{12} & -1 - A_2 R_{11} \end{pmatrix}, \tag{58}$$

where a_i are given in Eq. (50), R_{ij} are the expectation values of two $\perp_2$ fields explicitly given in Eqs. (E3) and (E4), and

$$A_1 = \frac{8\beta v^2(N-2)}{v^4 + 12\alpha\beta},\ A_2 = \frac{v^2(N-2)}{3\alpha}. \tag{59}$$

The derivation of H is given in Appendix E.

5. Comparison with numerical simulations

In this section we compare the distributions obtained for the spiked tensor in Sects. 3 and 4 with MC simulations. The method is basically the same as that taken in the previous works of the author [24–26]. Throughout this section we put $\alpha = 1/2$ without loss of generality. In the MC simulations, all the solutions to the eigenvector equation (1) must be computed for any randomly sampled C and η. Since this requires a reliable polynomial equation solver, we used Mathematica 13 for the MC simulations. It computes the solutions to Eq. (1), which are generally complex, among which we take only the real ones. To check whether all the solutions are covered, we checked whether the number of the generally complex solutions to Eq. (1) agreed with the number $2^N - 1$ of the generally complex eigenvectors proven in Ref. [13], every time the solutions were computed. In fact, when N is large, we encountered some cases that a few solutions were missing. However, the missing rates were too small to statistically be relevant for this study. For example, the missing rate was $\lesssim 10^{-4}$ in the $N = 9$ data we use in this paper. We used a workstation which had a Xeon W2295 (3.0GHz, 18 cores), 128GB DDR4 memory, and Ubuntu 20 as OS.

The MC simulations were performed by the following procedure.

- Randomly sample C and η. Each η_a is randomly sampled by the normal distribution with the mean value zero and the standard deviation $\sqrt{2\beta}$. Each C_{abc} is randomly sampled by the normal distribution with the mean value zero and the standard deviation $1/\sqrt{d_{abc}}$, corresponding to $\alpha = 1/2$, where d_{abc} is the degeneracy factor defined by[12]

$$d_{abc} = \begin{cases} 1 & \text{for } a = b = c, \\ 3 & \text{for } a \neq b = c \text{ or } b \neq c = a \text{ or } c \neq a = b, \\ 6 & \text{for } a \neq b \neq c \neq a. \end{cases} \tag{60}$$

- As explained above, compute all the complex solutions to the eigenvector equation (1), and pick up only the real ones v^i $(i = 1, 2, \cdots, \#\mathrm{sol}(Q, C, \eta))$.
- Store $\left(|v^i|, v^i \cdot n/|v^i|, \mathrm{sign}\left(\det M(v^i, Q, C)\right)\right)$ for $i = 1, 2, \cdots, \#\mathrm{sol}(Q, C, \eta)$.
- Repeat the above processes.

[12]This degeneracy factor is because the Gaussian term in Eq. (5) is $C_{abc}C_{abc} = \sum_{a\leq b\leq c=1}^{N} d_{abc} C_{abc}^2$ in terms of the independent components of the symmetric tensor C.

By this sampling procedure, we obtain a series of data, $\left(|v^h|, v^h \cdot n/|v^h|, \mathrm{sign}\left(\det M(v^h, Q, C)\right)\right)$ for $h = 1, 2, \cdots, L$, where L denotes the total number of real solutions obtained.[13]

To plot the distributions, we classify the data into equally spaced bins in v and angle θ as

$$
\begin{aligned}
& v - \delta_v/2 < v^h \leq v + \delta_v/2, \\
& \cos(\theta - \delta_\theta/2) < v^h \cdot n/|v^h| \leq \cos(\theta + \delta_\theta/2), \\
& \mathrm{sign}\left(\det M(v^h, Q, C)\right) = 1 \text{ or } \mathrm{sign}\left(\det M(v^h, Q, C)\right) = -1,
\end{aligned} \tag{61}
$$

where v, θ are the center values of a bin, and δ_v, δ_θ are the sizes of a bin. We denote the total number of data satisfying Eq. (61) as $\mathcal{N}_{\delta_v,\delta_\theta,+}(v,\theta)$ and $\mathcal{N}_{\delta_v,\delta_\theta,-}(v,\theta)$ for $\mathrm{sign}\left(\det M(v^h, Q, C)\right) = 1$ and $\mathrm{sign}\left(\det M(v^h, Q, C)\right) = -1$, respectively.

Then the distribution of the real eigenvectors from a set of data is given by

$$
\rho_{MC}(v, \theta; q, \beta) = \frac{1}{N_{\mathrm{MC}}\delta_v\delta_\theta}\left(\mathcal{N}_{\delta_v,\delta_\theta,+}(v,\theta) + \mathcal{N}_{\delta_v,\delta_\theta,-}(v,\theta) \pm \sqrt{\mathcal{N}_{\delta_v,\delta_\theta,+}(v,\theta) + \mathcal{N}_{\delta_v,\delta_\theta,-}(v,\theta)}\right), \tag{62}
$$

where N_{MC} denotes the total number of sampling processes in obtaining the data and the $\pm$ part represents error estimates. The signed distribution is given by

$$
\rho_{\mathrm{MC}}^{\mathrm{signed}}(v, \theta; q, \beta) = \frac{1}{N_{\mathrm{MC}}\delta_v\delta_\theta}\left(\mathcal{N}_{\delta_v,\delta_\theta,+}(v,\theta) - \mathcal{N}_{\delta_v,\delta_\theta,-}(v,\theta) \pm \sqrt{\mathcal{N}_{\delta_v,\delta_\theta,+}(v,\theta) + \mathcal{N}_{\delta_v,\delta_\theta,-}(v,\theta)}\right). \tag{63}
$$

As for the analytical side, since we take only the size $|v|$ and the relative angle θ as data, the above MC distributions should be compared with

$$
\begin{aligned}
\rho_{\mathrm{analy}}(v, \theta; q, \beta) dv d\theta &= \int_{|v'|=v,\ v'\cdot n/|v'|=\cos(\theta)} d^N v' \rho(v', q, n, \beta) \\
&= S_{N-2} v^{N-1} \sin^{N-2}(\theta)\, \rho(v, q, n, \beta) dv d\theta,
\end{aligned} \tag{64}
$$

where $S_{N-2} = 2\pi^{(N-1)/2}/\Gamma[(N-1)/2]$ is the surface volume of a unit sphere in the $N-1$-dimensional flat space. Here $\rho(v, q, n, \beta)$ is one of the expressions obtained in Sects. 3 and 4, and v in the argument of ρ on the right-hand side abusively denotes an arbitrary vector v' which satisfies $|v'| = v$, $v' \cdot n/|v'| = \cos(\theta)$. In the following we will compare the MC and the analytical results.

Let us first consider the signed distribution. The analytical result is obtained by putting Eq. (26) with Eq. (28) into Eq. (64). Since the analytical result is an exact result, it should agree with the MC result within errors. In Fig. 1, we plot the MC result (63) for $N = 9$, $\beta = 10^{-4}$, $q = 10$ with $N_{\mathrm{MC}} = 4 \cdot 10^4$. As examples, the analytical and MC results are compared at two slices, one at $|v| = 0.105$ and the other at $\theta = \pi/2$, in the two panels of Fig. 2. They agree quite well within error estimates, supporting the validities of both the analytical and the MC computations.

As in Fig. 1 and the left panel of Fig. 2, an evident negative peak can be observed around $|v| \sim 0.1$ and $\theta \sim 0.5$. This peak approximately corresponds to an eigenvector $q^{-1}n_a$ of the background tensor $Q_{abc} = q\, n_a n_b n_c$. In fact, the location satisfies $|v| \sim q^{-1}$, while the angle is not strictly $\theta = 0$. The reason is that the volume factor in Eq. (64) contains $\sin^{N-2}(\theta)$, and pushes the peak away from $\theta = 0$. Because of the same reason, the other major structures are concentrated around $\theta = \pi/2$ in Fig. 1. A large-N limit which effectively vanishes this volume effect will be discussed in Sect. 6.

[13] Note that L is generally different from N_{MC} below.

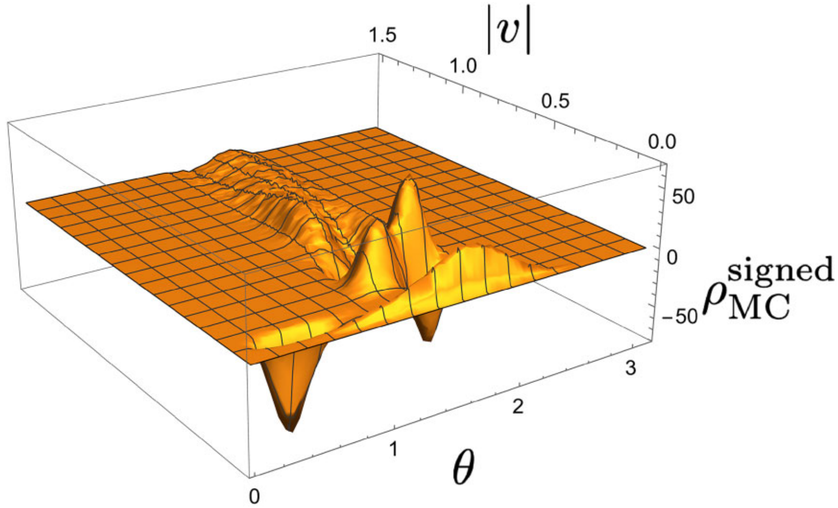

Fig. 1. The MC signed distribution (63) is plotted for the data with $N = 9$, $\beta = 10^{-4}$, $q = 10$ and total sampling number $N_{\mathrm{MC}} = 4 \cdot 10^4$.

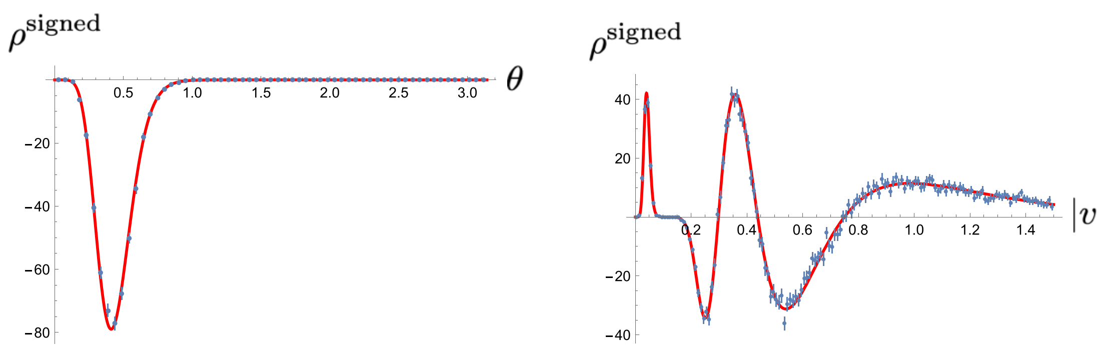

Fig. 2. The comparison between the analytical and the MC results with the same data as of Fig. 1. The analytical result is drawn by the solid lines and the MC results are plotted with error bars. The comparisons are shown for two example slices in $|v|$ and θ; the left is at $|v| = 0.105$ and the right is at $\theta = \pi/2$.

In Fig. 1 and the right panel of Fig. 2 one can also see a peak around $|v| \sim 0.04$, $\theta \sim \pi/2$. This peak corresponds to the trivial eigenvector $v = 0$. Because of $\beta > 0$ the distribution broadens around $|v| \sim 0$, and the volume factor v^{N-1} in Eq. (64) pushes the peak away from $|v| = 0$.

In Fig. 3 the MC distribution (62) is shown for the same data. Except for the signs, the characters of the distribution are more or less similar to the signed case. On the other hand, the analytic result for this case has the difference that the partition function Z in Eq. (35) is computed by the approximation (52), whereas it was exact for the signed case. The exact expression of $Z_{\perp_2}$ can be taken from the previous result in Ref. [26], which is explicitly given in Appendix F. As for $Z_{\parallel\perp_1}$, by numerically integrating Eq. (57) on a grid of points in $|v|$ and θ, an interpolation function of $Z_{\parallel\perp_1}$ is computed and used. In Fig. 4 the analytic and the MC results are compared. The agreement is fairly satisfactory except for some slight systematic deviations around a peak.

6. Large-N limit

In this section we will take large-N limits of the distribution obtained in Sect. 4.2 for a spiked tensor. We will particularly pay attention to the parameter region where the peak corresponding

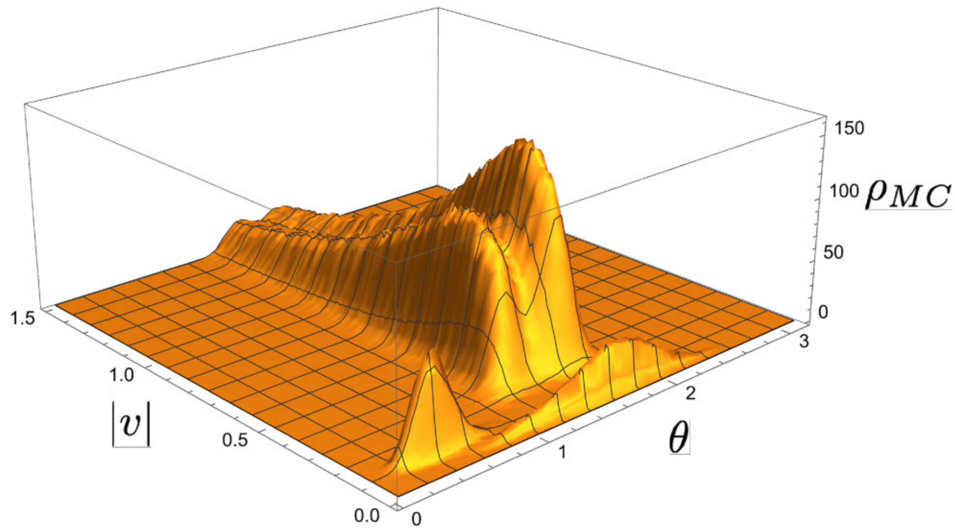

Fig. 3. The MC distribution (62) is plotted for the same data as used in Fig. 1 for $N = 9$, $\beta = 10^{-4}$, $q = 10$, and $N_{\mathrm{MC}} = 4 \cdot 10^4$.

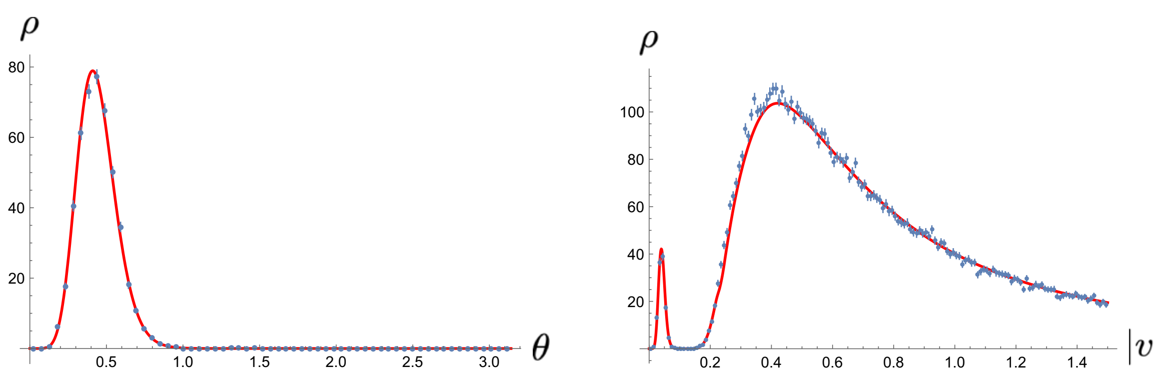

Fig. 4. The MC results are plotted with error bars for the same data as in Fig. 3. The analytic result is drawn by the solid lines. The left panel is of the slice at $|v| = 0.105$, and the right at $\theta = \pi/2$.

to the background Q can be seen in the eigenvector distribution. We will consider two large-N limits. In one large-N limit, we will derive the result that a peak can be well identified with Q for the parameter region, $\alpha q^2/N \gtrsim 0.6$, $\beta q^2 N \lesssim 0.1$. In particular for $\beta = 0$, we will find the threshold value to be $0.66 < (\alpha q^2/N)_c < 0.67$, which agrees with Proposition 2 of Ref. [29]. However, this peak is always smaller than the other peak(s) at $n_{\parallel} = 0$ and therefore relatively vanishes in the strict large-N limit. In the other scaling limit, $\alpha q^2 \sim N^{\gamma}$, $\beta q^2 \sim N^{-\gamma}$ with $\gamma > 1$, the peak remains in the strict large-N limit.

We want to consider large-N limits which keep both the parameters Q and β relevant. As was discussed in Sect. 5, the volume factor $\sin^{N-2}\theta$ in Eq. (64) suppresses the peak of the eigenvector $q^{-1}n$ of the background tensor Q, and this suppression becomes stronger as N becomes larger. Therefore, to obtain an interesting large-N limit, the parameters must be scaled so as to compete with $\sin^{N-2}\theta \sim e^{N\log(\sin\theta)}$. A large-$N$ scaling which makes the exponential factor in Eq. (41) of this order is given by

$$\alpha = \frac{N\tilde{\alpha}}{q^2}, \ \beta = \frac{\tilde{\beta}}{Nq^2}, \ v = \frac{\tilde{v}}{q}, \tag{65}$$

where $\tilde{\alpha}$, $\tilde{\beta}$ are kept finite. Here the factors of q are to absorb the dependence on q from the formulas below.

Let us discuss the large-N limit of $Z = Z_{\perp_2} Z_{\parallel\perp_1}$ in Sect. 4.2.4. The large-N limit of $Z_{\perp_2}$ was computed in Ref. [25], and it is given by

$$Z_{\perp_2}^{N=\infty} \sim \text{const.}\, e^{N S_{\perp_2}^{\infty}}, \tag{66}$$

where[14]

$$S_{\perp_2}^{\infty}(x) = \begin{cases} \log 2 + \log(x) + \frac{1-\sqrt{1-4x}}{4x} - \log\left(1 - \sqrt{1-4x}\right) & \text{for } 0 < x \leq \frac{1}{4}, \\ \frac{1}{4x} + \frac{1}{2}\log(x) & \text{for } \frac{1}{4} \leq x, \end{cases} \tag{67}$$

with[15] $x = (N-2)v^2/(3\alpha) \sim \tilde{v}^2/(3\tilde{\alpha})$. As for $Z_{\parallel\perp_1}$, one can easily see that the limit of Eq. (57) is just given by dropping the terms dependent on g_i in Eq. (50), while the N-dependencies of A_i in Eq. (59) and R_{ij} in Eqs. (E3) and (E4) drop out. Therefore, H does not depend on g_i and we get

$$Z_{\parallel\perp_1}^{N=\infty} = \pi^2 \sqrt{\det H}\Big|_{g_i=0}, \tag{68}$$

which has no relevant effects to the formula below for the large-N limit.

By collecting the results above and using Eqs. (64) and (41), we obtain

$$\begin{aligned} S_\infty(\tilde{v}, \theta) &= \lim_{N\to\infty} \frac{1}{N} \log \rho_{\text{analy}} \\ &= \text{const.} + S_{\perp_2}^{\infty} + \log \tilde{v} + \log(n_\perp) - \frac{1}{2}\log(\tilde{v}^4 + 12\tilde{\alpha}\tilde{\beta}) \\ &\quad + \frac{-\tilde{\alpha}\tilde{v}^2 + 2\tilde{\alpha}\tilde{v}^3 {n_\parallel}^3 - \tilde{\alpha}\tilde{v}^4 {n_\parallel}^6}{\tilde{v}^4 + 4\tilde{\alpha}\tilde{\beta}} - \frac{3\tilde{\alpha}\tilde{v}^4 {n_\parallel}^4 {n_\perp}^2}{\tilde{v}^4 + 12\tilde{\alpha}\tilde{\beta}}, \end{aligned} \tag{69}$$

where $n_\parallel = \cos\theta$ ($n_\perp = \sin\theta$), and const. is the part not dependent on $\tilde{v}$ or θ.

It is interesting to study the profile of $S_\infty(\tilde{v}, \theta)$ in the $\tilde{v}$ and θ plane for various values of $\tilde{\alpha}$, $\tilde{\beta}$. We have numerically studied it for the parameter region $10^{-3} \leq \tilde{\alpha} \leq 10^3$, $10^{-3} \leq \tilde{\beta} \leq 10^3$. In the unshaded region of Fig. 5, the peak(s) exist(s) only along $n_\parallel = 0$, as is shown in the left panel of Fig. 6 as an example. In the shaded region, in addition to the peak(s) at $n_\parallel = 0$, there exists also a peak which has nonzero $n_\parallel$. This peak corresponds to the eigenvector $q^{-1}n$ of the background tensor Q, as is shown in the right panel of Fig. 6 as an example. In Fig. 7, the values of $n_\parallel$ and $\tilde{v}$ are plotted for the latter peak. The location can be well identified with $q^{-1}n$, if the values take $n_\parallel \sim 1$ and $\tilde{v} \sim 1$. As can be seen in the plots, this occurs in the region, $\log_{10}\tilde{\alpha} \gtrsim -0.2$ and $\log_{10}\tilde{\beta} \lesssim -1$. This is the parameter region in which the background tensor Q can be detected well.

It is interesting to compare this detectable region with a result of Ref. [29]. As can be seen in Fig. 5, the shaded region has an edge around $\log_{10}\tilde{\alpha} \sim -0.2$, namely, $\tilde{\alpha} \sim 0.63$, independent of $\tilde{\beta}$ for $\log_{10}\tilde{\beta} \lesssim -1$. To see the threshold value more precisely for $\tilde{\beta} = 0$, we plot $n_\parallel$ and $\tilde{v}$ of the peak with $n_\parallel > 0$ in Fig. 8. We find that the peak does not exist at $\tilde{\alpha} \leq 0.66$, but exists at $\tilde{\alpha} \geq 0.67$ with $n_\parallel \gtrsim 0.7$. On the other hand, as explained in Appendix G, Proposition 2 of Ref. [29] states that the threshold value is $\tilde{\alpha} = 2/3$, which indeed agrees with our value.

[14] For simplicity, $S_{\perp_2}^{\infty}$ is shifted by an irrelevant constant from the corresponding expression with $R = 1/2$ in Ref. [25].

[15] N must be deducted by one, when we take a result from Ref. [25]. See a footnote below Eq. (E2).

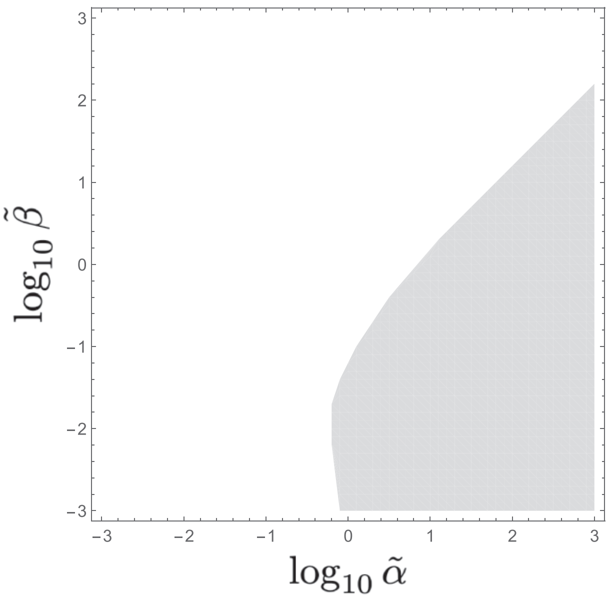

Fig. 5. In the shaded region of the parameters, the eigenvector distribution has a peak of S_∞ corresponding to the eigenvector of Q.

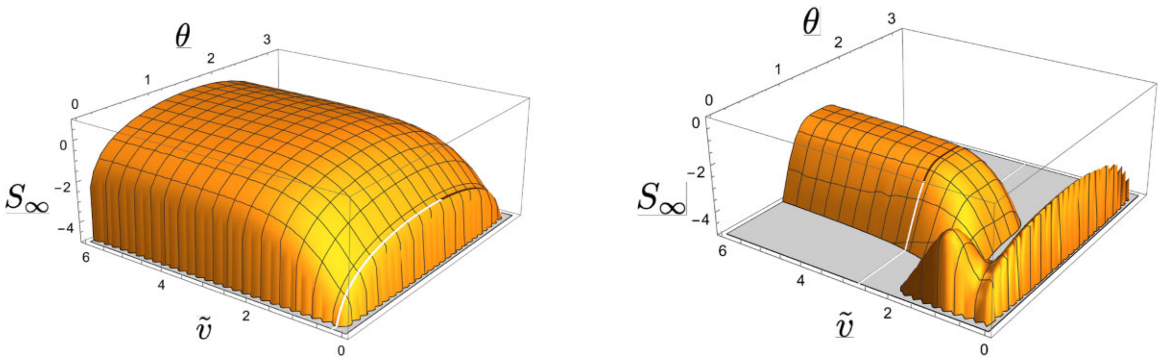

Fig. 6. In the left panel, S_∞ (const. being ignored) is plotted for $\log_{10}\tilde{\alpha} = -1$, $\log_{10}\tilde{\beta} = 1$, which is in the unshaded region of Fig. 5. The right panel is for $\log_{10}\tilde{\alpha} = 1$, $\log_{10}\tilde{\beta} = -2$ in the shaded region. In the latter case, a peak near $\tilde{v} \sim 1, \theta \sim 0$ corresponding to the eigenvector of Q can be found. The tiny gaps in the plots are not essential; they seem to be caused by the drawing program (Mathematica) avoiding the singularity at $x = 1/4$ in Eq. (67), where the function is continuous but its first derivative is discrete.

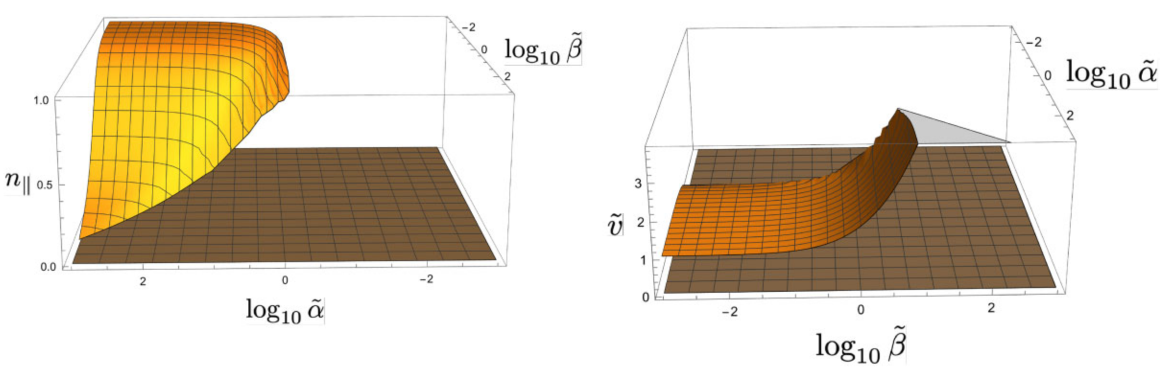

Fig. 7. The values of $n_\parallel$ (left) and $\tilde{v}$(right) of the peak with $n_\parallel > 0$, corresponding to the eigenvector of Q, are plotted. Identification of this peak with Q can well be done in the region $\log_{10}\tilde{\alpha} \gtrsim -0.2$ and $\log_{10}\tilde{\beta} \lesssim -1$.

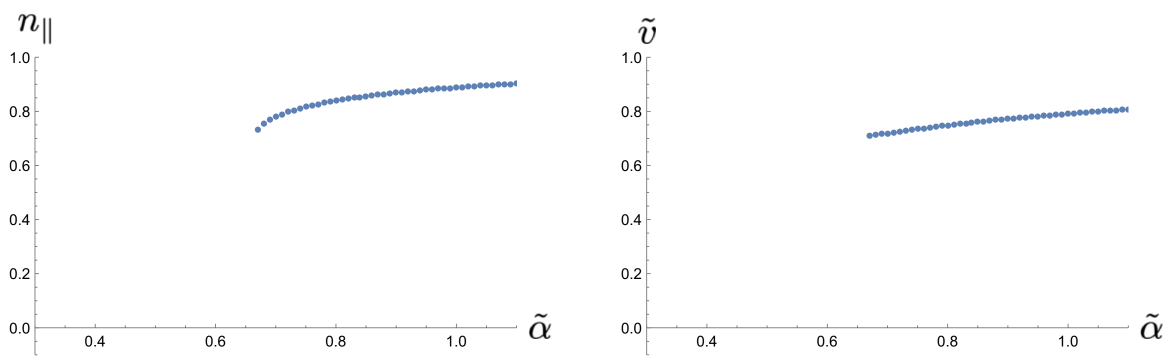

Fig. 8. The values of $n_\parallel$ and $\tilde{v}$ of the peak with $n_\parallel > 0$ for $\tilde{\beta} = 0$. The threshold value is $0.66 < \tilde{\alpha}_c < 0.67$.

We numerically observed that a peak at $n_\parallel = 0$ always takes the largest value of S_∞ at least in the parameter region of $\tilde{\alpha}, \tilde{\beta}$ we have studied above. This means that, because $\rho \sim e^{NS_\infty}$, the peak corresponding to Q will effectively be invisible compared to the peak(s) at $n_\parallel = 0$ in the strict large-N limit. Therefore, in the strict large-N limit, Q, namely a "signal," cannot be detected by solving the eigenvector equation (1).

The main reason for the above difficulty of detection comes from the strong effect of the volume factor $\sin^{N-2}\theta$ in Eq. (64), which enhances the region $n_\parallel \sim 0$ so strongly. Therefore, an obvious way to solve this difficulty is to consider another scaling limit which overwhelms the volume factor. An example is given by

$$\alpha = \frac{N^\gamma \tilde{\alpha}}{q^2},\ \beta = \frac{\tilde{\beta}}{N^\gamma q^2},\ v = \frac{\tilde{v}}{q},\ \gamma > 1. \tag{70}$$

In this limit, $x = (N-2)v^2/(3\alpha) \sim N^{-\gamma+1} \to 0$ in the large-N limit, so therefore Eq. (67) becomes a constant, meaning that $Z_{\perp_2}$ is a free theory independent of v. As for $Z_{\parallel\perp_1}$, $A_i \to 0$ and R_{ij} approaches finite values, so $Z_{\parallel\perp_1}$ is again a finite quantity. Therefore, from Eq. (41), the major contribution comes only from the exponent, and we obtain

$$\begin{aligned} S_\infty^\gamma(\tilde{v}, \theta) &= \lim_{N\to\infty} \frac{1}{N^\gamma} \log \rho_{\text{analy}} \\ &= \frac{-\tilde{\alpha}\tilde{v}^2 + 2\tilde{\alpha}\tilde{v}^3 {n_\parallel}^3 - \tilde{\alpha}\tilde{v}^4 {n_\parallel}^6}{\tilde{v}^4 + 4\tilde{\alpha}\tilde{\beta}} - \frac{3\tilde{\alpha}\tilde{v}^4 {n_\parallel}^4 {n_\perp}^2}{\tilde{v}^4 + 12\tilde{\alpha}\tilde{\beta}}. \end{aligned} \tag{71}$$

As is shown in Appendix H, it is straightforward to prove that the maximum value of S_∞^γ is 0, and this occurs only at three locations: (i) $\tilde{v} = 0$, (ii) $\tilde{v} \to \infty, n_\parallel = 0$, (iii) $\tilde{v} = 1, n_\parallel = 1$. The last location corresponds to the background Q. An example of S_∞^γ is shown in Fig. 9. Since the eigenvector distribution is given by $\rho \sim e^{N^\gamma S_\infty^\gamma}$, there remain only the three locations above in the strict large-N limit. This means that, in the limit, a finite eigenvector ($v \neq 0, \infty$) is surely that of the background Q.

7. Summary and future prospects

In this paper we have studied the real eigenvector distributions of real symmetric order-three Gaussian random tensors in the case that the random tensors have nonzero mean value backgrounds and the eigenvector equations have Gaussian random deviations. This is an extension of the previous studies [24–26], which have no such mean values or deviations. We have derived the quantum field theories with quartic interactions whose partition functions give the distributions. For the background tensor being rank-one (a spiked tensor case) in particular, we have

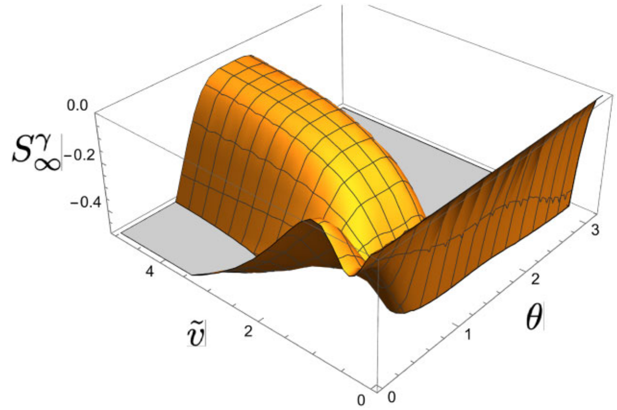

Fig. 9. S^{γ}_{∞} is plotted for $\log_{10}\tilde{\alpha} = 0$ and $\log_{10}\tilde{\beta} = -1$ as an example. There is a peak corresponding to the eigenvector of the background tensor Q.

explicitly derived the distributions by computing the partition functions exactly or approximately. We have obtained good agreement between the analytical results and MC simulations. We have derived the scaling and range of parameters for the background tensor to be detectable in the distributions in the large-N limit. Our threshold value has agreed with that of Ref. [29].

The quantum field theories we have derived in this paper are much more complicated than those in the previous studies [24–26] due to the presence of the backgrounds and the deviations. Nonetheless, we have obtained some exact expressions for the signed distributions, and have also derived some approximate expressions of the (authentic) distributions, which agree very well with the MC results. This success can be ascribed to the quantum field theoretical expressions, to which we can apply various well-developed techniques and knowledge of quantum field theories. The results of this paper strengthen our belief that the quantum field theoretical procedure for computing distributions of quantities in random tensors is general, powerful, and intuitive.

As far as random tensors are Gaussian, it is in principle straightforward to extend the quantum field theoretical procedure to some other problems in random tensors: distributions of complex eigenvectors/values, tensor rank decompositions, correlations among eigenvectors, etc. Although derived quantum field theories with quartic interactions may become quite complicated, it will always be possible to find ways to, exactly or approximately, compute the partition functions by quantum field theoretical techniques, knowledge, and intuition. These studies will enrich fundamental knowledge about random tensors, which will eventually be applied in various subjects in future studies.

Tensor models have emerged from discrete approaches to quantum gravity [6–9], and are also taking active part in more recent approaches, such as in the AdS/CFT correspondence [33]. A question of the author's interest is whether there exists in tensor models a phenomenon analogous to the Gross-Witten-Wadia transition [4,5]. In fact, there are some indications that similar transitions exist in the context of a discrete model of quantum gravity [34,35]. We hope the knowledge about random tensors enriched along the line of our studies will give some insights into quantum gravity in the future.

Acknowledgements

N.S. is supported in part by Japan Society for the Promotion of Science (JSPS) KAKENHI Grant No. 19K03825. He would like to thank M. Akyazi, N. Delporte, O. Evnin, R. Gurau, L. Lionni, Z. Mirzaiyan, and R. Toriumi for some stimulating discussions.

Funding

Open Access funding: SCOAP^3.

Appendix A. Derivation of Eq. (22)

From Eq. (14), the parallel/transverse parts of D^{signed} are given by

$$D_{\parallel}^{\text{signed}} = \frac{v^3}{\alpha}\bar{\psi}_{\parallel}\psi_{\parallel},$$
$$D_{\perp}^{\text{signed}} = \frac{v^3}{3\alpha}\left(\bar{\psi}_{\perp}\psi_{\parallel} + \bar{\psi}_{\parallel}\psi_{\perp}\right). \tag{A1}$$

By putting Eq. (A1) into Eq. (19), we obtain

$$\begin{aligned}\delta S_{\lambda}^{\text{signed}} - \delta S_{\lambda}^{\text{signed}}(Q=\beta=0) = &\frac{1}{2}\log b_{\parallel} + \frac{N-1}{2}\log b_{\perp} - \frac{\alpha(b_{\parallel}-1)}{v^2} + \frac{2\alpha b_{\parallel} D_{\parallel}^{Q}}{v^3} - \frac{\alpha b_{\parallel}\left(D_{\parallel}^{Q}\right)^2}{v^4}\\ &- \frac{3\alpha b_{\perp} D_{\perp}^{Q}\cdot D_{\perp}^{Q}}{v^4} - 2\left(b_{\parallel} - 1 - \frac{b_{\parallel} D_{\parallel}^{Q}}{v}\right)\bar{\psi}_{\parallel}\psi_{\parallel}\\ &+ \frac{2b_{\perp}}{v} D_{\perp}^{Q}\cdot\left(\bar{\psi}_{\perp}\psi_{\parallel} + \bar{\psi}_{\parallel}\psi_{\perp}\right) + \frac{2v^2(b_{\perp}-1)}{3\alpha}\bar{\psi}_{\parallel}\psi_{\parallel}\bar{\psi}_{\perp}\cdot\psi_{\perp}.\end{aligned} \tag{A2}$$

Adding this and the last term of Eq. (12) to Eq. (21), one obtains Eq. (22) with Eq. (23).

Appendix B. Derivation of Eq. (28)

Let us parametrize Eq. (27) as follows:

$$\begin{aligned}S_{b,d,k} = &b_1\bar{\psi}_{\parallel}\psi_{\parallel} + b_2\left(\bar{\psi}_{\parallel}\psi_{\perp_1} + \bar{\psi}_{\perp_1}\psi_{\parallel}\right) + b_3\bar{\psi}_{\perp_1}\psi_{\perp_1} + k\bar{\psi}_{\perp_2}\psi_{\perp_2}\\ &+ d_1\left(\bar{\psi}_{\perp_1}\psi_{\perp_1} + \bar{\psi}_{\perp_2}\psi_{\perp_2}\right)\bar{\psi}_{\parallel}\psi_{\parallel} + d_2\left(\bar{\psi}_1\psi_{\perp_1} + \bar{\psi}_{\perp_2}\psi_{\perp_2}\right)^2.\end{aligned} \tag{B1}$$

Then by explicitly performing the fermion integrations for $\parallel$ and $\perp_1$ directions, we obtain

$$\begin{aligned}&\int d\bar{\psi}d\psi\, e^{S_{b,d,k}}\\ &= \int d\bar{\psi}_{\perp_2}d\psi_{\perp_2}\left(d_1 + b_1b_3 - b_2^2 + (2b_1d_2 + b_3d_1)\bar{\psi}_{\perp_2}\cdot\psi_{\perp_2} + 2d_1d_2\left(\bar{\psi}_{\perp_2}\cdot\psi_{\perp_2}\right)^2\right)\\ &\quad\times e^{k\bar{\psi}_{\perp_2}\cdot\psi_{\perp_2} + d_2\left(\bar{\psi}_{\perp_2}\cdot\psi_{\perp_2}\right)^2}\\ &= \left(d_1 + b_1b_3 - b_2^2 + (2b_1d_2 + b_3d_1)\frac{\partial}{\partial k} + 2d_1d_2\frac{\partial^2}{\partial k^2}\right)\int d\bar{\psi}_{\perp_2}d\psi_{\perp_2}\, e^{k\bar{\psi}_{\perp_2}\cdot\psi_{\perp_2} + d_2\left(\bar{\psi}_{\perp_2}\cdot\psi_{\perp_2}\right)^2}.\end{aligned} \tag{B2}$$

Now the last fermion integration can be computed as

$$\begin{aligned}\int d\bar{\psi}_{\perp_2} d\psi_{\perp_2}\, e^{k\bar{\psi}_{\perp_2}\cdot\psi_{\perp_2}+d_2\left(\bar{\psi}_{\perp_2}\cdot\psi_{\perp_2}\right)^2} &= \sum_{n=0}^{\infty}\frac{d_2^n}{n!}\left(\bar{\psi}_{\perp_2}\cdot\psi_{\perp_2}\right)^{2n}\int d\bar{\psi}_{\perp_2} d\psi_{\perp_2}\, e^{k\bar{\psi}_{\perp_2}\cdot\psi_{\perp_2}} \\ &= \sum_{n=0}^{\lfloor\frac{N-2}{2}\rfloor}\frac{d_2^n}{n!}\frac{\partial^{2n}}{\partial k^{2n}}k^{N-2} \\ &= (-4d_2)^{\frac{N-3}{2}}k\,U\left(\frac{3-N}{2},\frac{3}{2},-\frac{k^2}{4d_2}\right), \end{aligned} \tag{B3}$$

where U is the confluent hypergeometric function of the second kind. The last equality can be shown by using the following relation to a hypergeometric function and comparing with its asymptotic expansion:

$$U(a,b,z)\sim z^{-a}\,{}_2F_0(a,1+a-b,-z^{-1}), \tag{B4}$$

where the hypergeometric function has a formal series expansion,

$${}_2F_0(a,b,x)=\sum_{n=0}^{\infty}\frac{(a)_n(b)_n}{n!}x^n \tag{B5}$$

with the Pochhammer symbol, $(a)_n = a(a+1)\cdots(a+n-1)$ ($(a)_0=1$). For the argument in Eq. (B3), the formal series stops at finite n, and hence Eq. (B4) is an exact relation. One can also find that the confluent hypergeometric function here can be expressed by a hermite polynomial.

Appendix C. Explicit form of S_0

The $Q=\beta=0$ case was studied in Ref. [26], and the action for this case is given by

$$S_0 = K_F + K_B + V_F + V_B + V_{BF}, \tag{C1}$$

where

$$\begin{aligned} K_F &= -\bar{\varphi}_\perp\cdot\varphi_\perp - \bar{\psi}_\perp\cdot\varphi_\perp - \bar{\varphi}_\perp\cdot\psi_\perp + \epsilon\bar{\psi}_\perp\cdot\psi_\perp - \bar{\varphi}_\parallel\cdot\varphi_\parallel + \bar{\psi}_\parallel\cdot\varphi_\parallel + \bar{\varphi}_\parallel\cdot\psi_\parallel + \epsilon\bar{\psi}_\parallel\cdot\psi_\parallel, \\ K_B &= -{\sigma_\perp}^2 - 2i\sigma_\perp\cdot\phi_\perp - \epsilon{\phi_\perp}^2 - {\sigma_\parallel}^2 + 2i\sigma_\parallel\cdot\phi_\parallel - \epsilon{\phi_\parallel}^2, \\ V_F &= -\frac{v^2}{6\alpha}\left((\bar{\psi}_\perp\cdot\varphi_\perp)^2 + (\bar{\varphi}_\perp\cdot\psi_\perp)^2 + 2\bar{\psi}_\perp\cdot\bar{\varphi}_\perp\varphi_\perp\cdot\psi_\perp + 2\bar{\psi}_\perp\cdot\psi_\perp\bar{\varphi}_\perp\cdot\varphi_\perp\right), \\ V_B &= -\frac{2v^2}{3\alpha}\left({\sigma_\perp}^2{\phi_\perp}^2 + (\sigma_\perp\cdot\phi_\perp)^2\right), \\ V_{BF} &= \frac{2iv^2}{3\alpha}\left(\bar{\psi}_\perp\cdot\sigma_\perp\varphi_\perp\cdot\phi_\perp + \bar{\varphi}_\perp\cdot\sigma_\perp\psi_\perp\cdot\phi_\perp + \bar{\psi}_\perp\cdot\phi_\perp\varphi_\perp\cdot\sigma_\perp + \bar{\varphi}_\perp\cdot\phi_\perp\psi_\perp\cdot\sigma_\perp\right). \end{aligned} \tag{C2}$$

Note that the kinetic terms of the parallel and the transverse components of the fields respectively have slightly different sign structures, and that the four-interactions exist only among the transverse components.

Appendix D. Distribution for $N = 1$ rank-one Q

In this appendix, we derive Eq. (44). Ignoring all the transverse components, and setting $n_{\|} = 1$ in Eqs. (35), (39), (43), and (C2), we obtain

$$\rho(v, q, \beta) = \pi^{-2}\alpha^{\frac{1}{2}}(v^4 + 12\alpha\beta)^{-\frac{1}{2}} \exp\left[\frac{-\alpha v^2 + 2\alpha q v^3 - \alpha q^2 v^4}{v^4 + 4\alpha\beta}\right](-1)\int dgd\bar{\psi}\cdots d\sigma\, e^{S_{N=1}}, \tag{D1}$$

where

$$S_{N=1} = -g^2 - \bar{\varphi}_{\|}\cdot\varphi_{\|} + (a + bg)(\bar{\psi}_{\|}\cdot\varphi_{\|} + \bar{\varphi}_{\|}\cdot\psi_{\|}) + \epsilon\bar{\psi}_{\|}\cdot\psi_{\|} - {\sigma_{\|}}^2 + 2i(a + bg)\sigma_{\|}\cdot\phi_{\|} - \epsilon{\phi_{\|}}^2 \tag{D2}$$

with a, b given in Eq. (45).

The boson–fermion integration in Eq. (D1) produces a square root of the determinant of a two-by-two matrix. It is easy to see that the $\epsilon \to +0$ limit is smooth, and we obtain

$$\begin{aligned}(-1)\int dgd\bar{\psi}\cdots d\sigma\, e^{S_{N=1}} &= \pi\int dg\, e^{-g^2}\,|a + bg| \\ &= \pi\left(\sqrt{\pi}\,a\,\mathrm{Erf}\left(\frac{a}{b}\right) + b\,e^{-\frac{a^2}{b^2}}\right)\end{aligned} \tag{D3}$$

with the error function Erf.

Appendix E. Interactions between the $\|\perp_1$ and $\perp_2$ fields

There are no quadratic terms containing one $\|\perp_1$ field and one $\perp_2$ field, because the index of the $\perp_2$ field cannot be contracted with v or n. Therefore, the $\|\perp_1$ fields can couple with the $\perp_2$ fields only through the four-interaction terms in Eqs. (42) and (C2). By noting that $X_\perp \cdot Y_\perp = X_{\perp_1}Y_{\perp_1} + X_{\perp_2}\cdot Y_{\perp_2}$ for arbitrary fields X, Y, and collecting all the interaction terms between the $\|\perp_1$ and the $\perp_2$ fields, we obtain

$$V_{\|\perp_1,\perp_2} = \frac{8\beta v^2}{v^4+12\alpha\beta}\big(\bar\psi_{\perp_2}\cdot\bar\varphi_{\perp_2}\psi_\|\varphi_\| + \psi_{\perp_2}\cdot\varphi_{\perp_2}\bar\psi_\|\bar\varphi_\| - \bar\psi_{\perp_2}\cdot\psi_{\perp_2}\bar\varphi_\|\varphi_\|$$
$$- \bar\psi_{\perp_2}\cdot\varphi_{\perp_2}\bar\psi_\|\varphi_\| - \bar\varphi_{\perp_2}\cdot\varphi_{\perp_2}\bar\psi_\|\psi_\| - \bar\varphi_{\perp_2}\cdot\psi_{\perp_2}\bar\varphi_\|\psi_\|\big)$$
$$+ \frac{16\beta v^2 i}{v^4+12\alpha\beta}\left(\bar\psi_{\perp_2}\varphi_\| + \bar\psi_\|\varphi_{\perp_2} + \bar\varphi_{\perp_2}\psi_\| + \bar\varphi_\|\psi_{\perp_2}\right)\left(\sigma_\|\phi_{\perp_2} + \sigma_{\perp_2}\phi_\|\right)$$
$$- \frac{16\beta v^2}{v^4+12\alpha\beta}\left({\sigma_\|}^2\phi_{\perp_2}\cdot\phi_{\perp_2} + {\phi_\|}^2\sigma_{\perp_2}\cdot\sigma_{\perp_2} + 2\sigma_\|\phi_\|\phi_{\perp_2}\cdot\sigma_{\perp_2}\right)$$
$$- \frac{v^2}{3\alpha}\big(\bar\psi_{\perp_2}\cdot\varphi_{\perp_2}\bar\psi_{\perp_1}\varphi_{\perp_1} + \bar\varphi_{\perp_2}\cdot\psi_{\perp_2}\bar\varphi_{\perp_1}\psi_{\perp_1} + \bar\psi_{\perp_1}\bar\varphi_{\perp_1}\varphi_{\perp_2}\cdot\psi_{\perp_2}$$
$$+ \bar\psi_{\perp_2}\cdot\bar\varphi_{\perp_2}\varphi_{\perp_1}\psi_{\perp_1} + \bar\psi_{\perp_1}\psi_{\perp_1}\bar\varphi_{\perp_2}\cdot\varphi_{\perp_2} + \bar\psi_{\perp_2}\cdot\psi_{\perp_2}\bar\varphi_{\perp_1}\varphi_{\perp_1}\big)$$
$$- \frac{2v^2}{3\alpha}\left({\sigma_{\perp_1}}^2{\phi_{\perp_2}}^2 + {\sigma_{\perp_2}}^2{\phi_{\perp_1}}^2 + 2\sigma_{\perp_2}\cdot\phi_{\perp_2}\sigma_{\perp_1}\phi_{\perp_1}\right)$$
$$+ \frac{2v^2 i}{3\alpha}\big(\bar\psi_{\perp_1}\sigma_{\perp_1}\varphi_{\perp_2}\cdot\phi_{\perp_2} + \bar\psi_{\perp_2}\cdot\sigma_{\perp_2}\varphi_{\perp_1}\phi_{\perp_1} + \bar\varphi_{\perp_1}\sigma_{\perp_1}\psi_{\perp_2}\cdot\phi_{\perp_2}$$
$$+ \bar\varphi_{\perp_2}\cdot\sigma_{\perp_2}\psi_{\perp_1}\phi_{\perp_1} + \bar\psi_{\perp_1}\phi_{\perp_1}\varphi_{\perp_2}\cdot\sigma_{\perp_2} + \bar\psi_{\perp_2}\cdot\phi_{\perp_2}\varphi_{\perp_1}\sigma_{\perp_1}$$
$$+ \bar\varphi_{\perp_1}\phi_{\perp_1}\psi_{\perp_2}\cdot\sigma_{\perp_2} + \bar\varphi_{\perp_2}\cdot\phi_{\perp_2}\psi_{\perp_1}\sigma_{\perp_1}\big). \tag{E1}$$

The expectation values of the $\perp_2$ fields can be taken from the large-N Schwinger–Dyson analysis performed in Ref. [25]. The results were[16]

$$\langle\bar\psi_{\perp_2 a}\psi_{\perp_2 b}\rangle = R_{11}\delta_{ab},$$
$$\langle\bar\psi_{\perp_2 a}\varphi_{\perp_2 b}\rangle = R_{12}\delta_{ab},$$
$$\langle\bar\varphi_{\perp_2 a}\psi_{\perp_2 b}\rangle = R_{21}\delta_{ab},$$
$$\langle\bar\varphi_{\perp_2 a}\varphi_{\perp_2 b}\rangle = R_{22}\delta_{ab},$$
$$\text{Others} = 0, \tag{E2}$$

where, with a newly introduced parameter[17] $x = v^2(N-2)/(3\alpha)$,

[16] To avoid duplication of notations, we use R_{ij} in place of Q_{ij} of Ref. [25]. Another thing to note is that, though we have both bosons and fermions in the current system, which is different from the setup of Ref. [25], the leading-order Schwinger–Dyson analysis of the current system turns out to lead to the same two-fermion expectation values as in Ref. [25]. The reason is the presence of the supersymmetry explained below, which assures the two-boson expectation values are just copies of those of fermions.

[17] As the dimension of $\perp_2$ is $N-2$, the formula presented in Ref. [25] for the dimension $N-1$ of $\perp$ must be replaced with $N-2$.

- $0 < x < 1/4$

$$R_{11} = \frac{-\sqrt{1-4x}+1}{2x\sqrt{1-4x}},$$

$$R_{12} = R_{21} = \frac{1-\sqrt{1-4x}-4x}{2x\sqrt{1-4x}},$$

$$R_{22} = 0, \tag{E3}$$

- $x > 1/4$

$$R_{11} = \frac{\sqrt{-1+4x}}{2\sqrt{\epsilon}x} - \frac{1}{2x} + \mathcal{O}(\sqrt{\epsilon}),$$

$$R_{12} = R_{21} = -\frac{1}{2x} + \frac{\sqrt{\epsilon}}{2x\sqrt{-1+4x}} + \mathcal{O}(\epsilon^{\frac{3}{2}}),$$

$$R_{22} = -\frac{\sqrt{\epsilon}\sqrt{-1+4x}}{2x} + \frac{\epsilon}{2x} + \mathcal{O}(\epsilon^{\frac{3}{2}}). \tag{E4}$$

The two-boson expectation values can also be represented by R_{ij} by assuming that a supersymmetry is not spontaneously broken. It is easy to check that $S_0 + S_{Q,\beta}$ from Eqs. (C1) and (37) are invariant under the following supersymmetry transformation:

$$\delta\psi_a = -\phi_a,\ \delta\phi_a = \frac{1}{2}\bar{\psi}_a,\ \delta\varphi_a = i\sigma_a,\ \delta\sigma_a = \frac{i}{2}\bar{\varphi}_a,\ \delta(\text{others}) = 0. \tag{E5}$$

By assuming the nonbreaking of the supersymmetry, we obtain e.g. a relation, $0 = \langle\delta(\psi_a\sigma_b)\rangle = -\langle\phi_a\sigma_b\rangle - \langle\psi_a\frac{i}{2}\bar{\varphi}_b\rangle$. From such relations, we obtain

$$\langle\phi_a\phi_b\rangle = \frac{1}{2}R_{11}\delta_{ab},$$

$$\langle\phi_a\sigma_b\rangle = \frac{i}{2}R_{21}\delta_{ab},$$

$$\langle\sigma_a\phi_b\rangle = \frac{i}{2}R_{12}\delta_{ab},$$

$$\langle\sigma_a\sigma_b\rangle = -\frac{1}{2}R_{22}\delta_{ab}. \tag{E6}$$

Here, because ϕ, σ are bosons, the second and the third relations require $R_{12} = R_{21}$, which indeed holds in Eqs. (E3) and (E4).

By putting Eqs. (E2) and (E6) into Eq. (E1), we obtain

$$\begin{aligned} V_{\|\perp_1,\perp_2}(R) = &-A_1\left(R_{22}\bar{\psi}_\|\psi_\| + R_{12}(\bar{\psi}_\|\varphi_\| + \bar{\varphi}_\|\psi_\|) + R_{11}\bar{\varphi}_\|\varphi_\|\right) \\ &+ A_1\left(R_{22}{\phi_\|}^2 - 2iR_{12}\phi_\|\sigma_\| - R_{11}{\sigma_\|}^2\right) \\ &- A_2\left(R_{22}\bar{\psi}_{\perp_1}\psi_{\perp_1} + R_{12}(\bar{\psi}_{\perp_1}\varphi_{\perp_1} + \bar{\varphi}_{\perp_1}\psi_{\perp_1}) + R_{11}\bar{\varphi}_{\perp_1}\varphi_{\perp_1}\right) \\ &+ A_2\left(R_{22}{\phi_{\perp_1}}^2 - 2iR_{12}\phi_{\perp_1}\sigma_{\perp_1} - R_{11}{\sigma_{\perp_1}}^2\right), \end{aligned} \tag{E7}$$

where A_i are given in Eq. (59). Adding Eq. (E7) to Eq. (49), we obtain the full kinetic terms of the $\|\perp_1$ fields. In particular the fermionic part has the form,

$$K_{\|\perp_1} + V_{\|\perp_1,\perp_2}(R) = \bar{\psi}_{\|\perp_1}H\psi_{\|\perp_1} + \text{bosonic part}, \tag{E8}$$

where $\bar{\psi}_{\parallel\perp_1} = (\bar{\psi}_\parallel, \bar{\varphi}_\parallel, \bar{\psi}_{\perp_1}, \bar{\varphi}_{\perp_1})$, $\psi_{\parallel\perp_1} = (\psi_\parallel, \varphi_\parallel, \psi_{\perp_1}, \varphi_{\perp_1})$, and H is given in Eq. (58). Because of the supersymmetry, the bosonic part has essentially a parallel structure as H.

Appendix F. Exact expression of $Z_{\perp_2}$

$Z_{\perp_2}$ can be taken from Ref. [26], because it is the same as the partition function of the transverse components of the fields in Ref. [26], which is denoted as G_N there. A point to note is that, while the dimension of the transverse directions there is $N-1$, the dimension of $\perp_2$ of this paper is $N-2$. Therefore we have to deduct N by one,[18] when we take a result from Ref. [26]. In our current case of $N=9$, this corresponds to $G_{N=8}$, and therefore

$$\begin{aligned} Z_{\perp_2}^{N=9} &= G_{N=8} \\ &= \pi^{\frac{13}{2}} \Bigg(\frac{\sqrt{2} e^{-\frac{1}{8z}} (1 + 210z^2 - 2100z^3 + 12600z^4 + 25200z^5)}{15 z^{\frac{3}{2}}} \\ &\quad + (1 - 42z + 420z^2 - 840z^3)\, \gamma\left[\frac{1}{2}, \frac{1}{8z}\right] \Bigg), \end{aligned} \tag{F1}$$

where $z = v^2/(6\alpha)$, and $\gamma[1/2, y]$ is the lower incomplete gamma function with index 1/2, which is related to the error function by

$$\gamma\left[\frac{1}{2}, y\right] = \sqrt{\pi}\, \mathrm{Erf}\left(\sqrt{y}\right). \tag{F2}$$

Appendix G. Proposition 2 of Ref. [29]

In this appendix we compare our threshold value $\tilde{\alpha}$ with the value given in Proposition 2 of Ref. [29].

In Ref. [29] with their notations, the random tensor Y with a background is given by

$$Y = \lambda u^{\otimes k} + \frac{1}{\sqrt{2N}} W, \tag{G1}$$

where $|u| = 1$, $W = \sum_\pi G^\pi / k!$ with $G_{i_1 \cdots i_k} \sim N(0, 1)$, and π denotes permutations. By taking $k = 3$ and computing the standard deviations of W_{abc}, we find

$$W_{abc} \sim N\left(0, 1/\sqrt{d_{abc}}\right), \tag{G2}$$

where d_{abc} is the degeneracy factor defined in Eq. (60). In our case, $C_{abc} \sim N(0, 1/\sqrt{2\alpha d_{abc}})$, and therefore

$$\alpha = N \tag{G3}$$

is taken in Ref. [29] in our notation. $q = \lambda$ is also taken. Therefore,

$$\tilde{\alpha} = \frac{\alpha q^2}{N} = \lambda^2. \tag{G4}$$

Proposition 2 states

$$\lambda_c^2 = \frac{(k-1)^{k-1}}{2k(k-2)^{k-2}} = \frac{2}{3} \tag{G5}$$

for $k = 3$. Therefore, the threshold value of Ref. [29] corresponds to $\tilde{\alpha}_c = 2/3$.

[18] See also the footnotes associated to Eqs. (53) and (E2).

Appendix H. Maximums of S^γ_∞

In this section we will prove that $S^\gamma_\infty < 0$ for $0 < \tilde{v} < \infty$ and $-1 \leq n_\parallel < 1$. Firstly,

$$\left(v^4 + 4\tilde{\alpha}\tilde{\beta}\right)\left(v^4 + 12\tilde{\alpha}\tilde{\beta}\right)S^\gamma_\infty = -\tilde{\alpha}\tilde{v}^2\left(\tilde{v}^4 - 2{n_\parallel}^3\tilde{v}^5 + \left(3{n_\parallel}^4 - 2{n_\parallel}^6\right)\tilde{v}^6 + 12\tilde{\alpha}\tilde{\beta}\left(1 - 2{n_\parallel}^3\tilde{v} + {n_\parallel}^4\tilde{v}^2\right)\right). \tag{H1}$$

Therefore, the statement is equivalent to proving the positivity of the quantity in the parentheses:

$$\begin{aligned}&\tilde{v}^4 - 2{n_\parallel}^3\tilde{v}^5 + \left(3{n_\parallel}^4 - 2{n_\parallel}^6\right)\tilde{v}^6 + 12\tilde{\alpha}\tilde{\beta}\left(1 - 2{n_\parallel}^3\tilde{v} + {n_\parallel}^4\tilde{v}^2\right)\\ &= \left(1 - 2{n_\parallel}^3\tilde{v} + {n_\parallel}^4\tilde{v}^2\right)\tilde{v}^4 + 2{n_\parallel}^4\left(1 - {n_\parallel}^2\right)\tilde{v}^6 + 12\tilde{\alpha}\tilde{\beta}\left(1 - 2{n_\parallel}^3\tilde{v} + {n_\parallel}^4\tilde{v}^2\right).\end{aligned} \tag{H2}$$

For $n_\parallel < 1$, we find

$$1 - 2{n_\parallel}^3\tilde{v} + {n_\parallel}^4\tilde{v}^2 > 1 - 2{n_\parallel}^2\tilde{v} + {n_\parallel}^4\tilde{v}^2 = \left(1 - {n_\parallel}^2\tilde{v}\right)^2 \geq 0. \tag{H3}$$

Similarly, one can prove that the quantities in the other parentheses are larger than zero.

References

[1] E. P. Wigner, Ann. Math. **67**, 325 (1958).
[2] E. Brezin, C. Itzykson, G. Parisi, and J. B. Zuber, Commun. Math. Phys. **59**, 35 (1978) .
[3] B. Eynard, Counting surfaces : CRM Aisenstadt chair lectures, Prog. Math. Phys. 70, (Birkhäuser, 2016).
[4] D. J. Gross and E. Witten, Phys. Rev. D **21**, 446 (1980) .
[5] S. R. Wadia, Phys. Lett. B **93**, 403 (1980).
[6] J. Ambjorn, B. Durhuus, and T. Jonsson, Mod. Phys. Lett. A **6**, 1133 (1991) .
[7] N. Sasakura, Mod. Phys. Lett. A **6**, 2613 (1991) .
[8] N. Godfrey and M. Gross, Phys. Rev. D **43**, R1749(R) (1991).
[9] R. Gurau, Commun. Math. Phys. **304**, 69 (2011) [arXiv:0907.2582 [hep-th]] [Search inSPIRE].
[10] M. Ouerfelli, V. Rivasseau, and M. Tamaazousti, [arXiv:2205.10326 [hep-th]] [Search inSPIRE].
[11] L. Qi, J. Symb. Comput. **40**, 1302 (2005).
[12] L. H. Lim, Singular values and eigenvalues of tensors: a variational approach,in Proceedings of the IEEE International Workshop on Computational Advances in Multi-Sensor Adaptive Processing (CAMSAP '05), Vol. **1** (IEEE, New York, 2005), p. 129.
[13] D. Cartwright and B. Sturmfels, Linear Algebra Appl. **438**, 942 (2013).
[14] L. Qi, H. Chen, and Y. Chen, Tensor Eigenvalues and Their Applications (Springer, Singapore, 2018).
[15] A. Crisanti and H.-J. Sommers, Z. Phys. B **87**, 341 (1992).
[16] T. Castellani and A. Cavagna, J. Stat. Mech. Theo. Exp. **2005**, P05012 (2005) [arXiv:cond-mat/0505032] [Search inSPIRE].
[17] A. Auffinger, G. Ben Arous, and J. Černý, Comm. Pure Appl. Math. **66**, 165 (2013) [arXiv:1003.1129 [math.PR]] [Search inSPIRE].
[18] A. Biggs, J. Maldacena, and V. Narovlansky, [arXiv:2309.08818 [hep-th]] [Search inSPIRE].
[19] O. Evnin, Class. Quant. Grav. **38**, 203001 (2021) [arXiv:2104.09797 [gr-qc]] [Search inSPIRE].
[20] P. Breiding, SIAM J. Appl. Algebra Geom. **1**, 254 (2017).
[21] P. Breiding, Trans. Am. Math. Soc. **372**, 7857 (2019).
[22] O. Evnin, Lett. Math. Phys. **111**, 66 (2021) [arXiv:2003.11220 [math-ph]] [Search inSPIRE].
[23] R. Gurau, [arXiv:2004.02660 [math-ph]] [Search inSPIRE].
[24] N. Sasakura, Phys. Lett. B **836**, 137618 (2023) [arXiv:2208.08837 [hep-th]] [Search inSPIRE].
[25] N. Sasakura, Prog. Theor. Exp. Phys. **2023**, 013A02 (2023) [arXiv:2209.07032 [hep-th]] [Search in SPIRE].
[26] N. Sasakura, J. Math. Phys. **64**, 063501 (2023) [arXiv:2210.15129 [hep-th]] [Search inSPIRE].
[27] A. Montanari and E. Richard, in Proceedings of Adv. in Neural Inf. Process. Syst. 27 (NIPS 2014),2014.

[28] T. Lesieur, L. Miolane, M. Lelarge, F. Krzakala, and L. Zdeborova, Statistical and computational phase transitions in spiked tensor estimation, in 2017 IEEE International Symposium on Information Theory (ISIT) (IEEE, New York, 2017), p. 511.
[29] G. Ben Arous, S. Mei, A. Montanari, and M. Nica, Commun. Pure Appl. Math. **72**, 2282 (2019).
[30] N. Delporte, N. Sasakura, and R. Toriumi, in preparation.
[31] J. Zinn-Justin, Quantum Field Theory and Critical Phenomena (Clarendon Press, Oxford, 1989).
[32] Y. V. Fyodorov and A. Nock, J. Stat. Phys. **159**, 731 (2015).
[33] E. Witten, J. Phys. A **52**, 474002 (2019) [arXiv:1610.09758 [hep-th]] [Search inSPIRE].
[34] T. Kawano and N. Sasakura, Prog. Theor. Exp. Phys. **2022**, 043A01 (2022) [arXiv:2109.09896 [hep-th]] [Search inSPIRE].
[35] N. Sasakura, Phys. Rev. D **106**, 126016 (2022) [arXiv:2206.12017 [hep-th]] [Search inSPIRE].